

AD-A051 497

NEW YORK UNIV N Y DEPT OF APPLIED SCIENCE

F/G 20/4

THE EFFECTS OF ACOUSTICAL DISTURBANCES ON BOUNDARY LAYER TRANSI--ETC(U)

JAN 78 G MILLER, A CALLEGARI

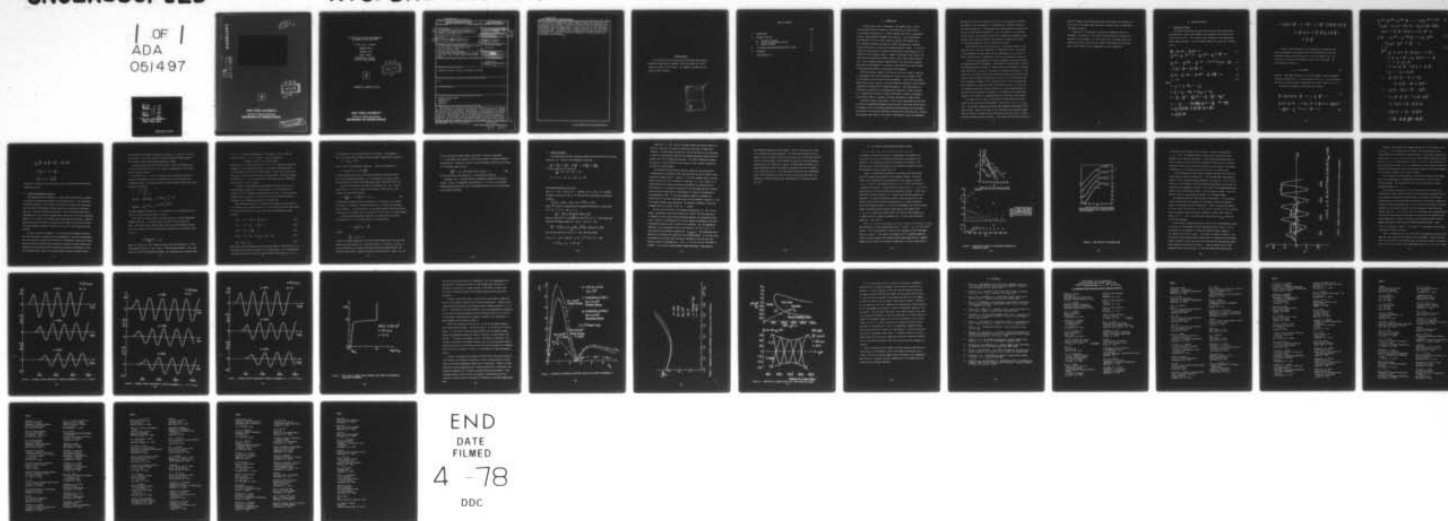
N00014-76-C-0183

UNCLASSIFIED

NYU/DAS-78/01

NL

1 OF 1  
ADA  
05/4 97

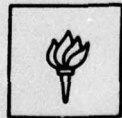
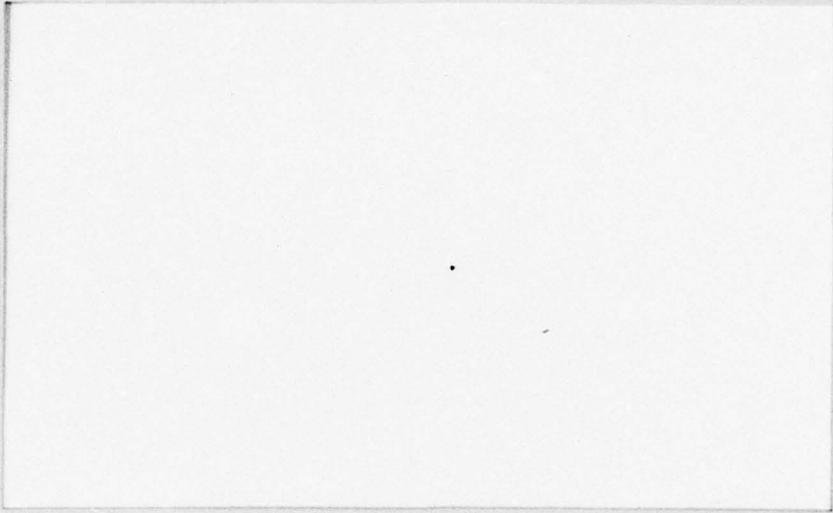


END  
DATE  
FILMED  
4 -78  
DDC

AD No. \_\_\_\_\_  
DDC FILE COPY

AD A 051497

(2) A



DDC  
RECEIVED  
MAR 20 1978  
F

NEW YORK UNIVERSITY  
FACULTY OF ARTS AND SCIENCE  
DEPARTMENT OF APPLIED SCIENCE

DISTRIBUTION STATEMENT A  
Approved for public release;  
Distribution Unlimited

THE EFFECTS OF ACOUSTICAL DISTURBANCES  
ON BOUNDARY LAYER TRANSITION

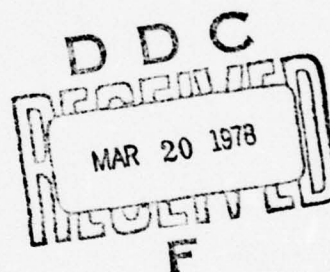
G. Miller and A. Callegari

NYU/DAS #78/01

JANUARY 1978

ANNUAL REPORT

DEPARTMENT OF THE NAVY  
OFFICE OF NAVAL RESEARCH



CONTRACT NO. N00014-76-C-0183

**NEW YORK UNIVERSITY**  
FACULTY OF ARTS AND SCIENCE  
**DEPARTMENT OF APPLIED SCIENCE**

Unclassified

SECURITY CLASSIFICATION OF THIS PAGE (When Data Entered)

REPORT DOCUMENTATION PAGE		READ INSTRUCTIONS BEFORE COMPLETING FORM	
1. REPORT NUMBER	2. GOVT ACCESSION NO.	3. RECIPIENT'S CATALOG NUMBER	
4. TITLE (and Subtitle) <b>THE EFFECTS OF ACOUSTICAL DISTURBANCES ON BOUNDARY LAYER TRANSITION.</b>		5. TYPE OF REPORT & PERIOD COVERED <b>Annual Technical Report.</b> 9/15/75 to 12/15/77 15 Sep 75-15 14 15 16 17 18 19 20 21 22 23 24 25 26 27 28 29 30 31 32 33 34 35 36 37 38 39 40 41 42 43 44 45 46 47 48 49 50 51 52 53 54 55 56 57 58 59 60 61 62 63 64 65 66 67 68 69 70 71 72 73 74 75 76 77 78 79 80 81 82 83 84 85 86 87 88 89 90 91 92 93 94 95 96 97 98 99 100 101 102 103 104 105 106 107 108 109 110 111 112 113 114 115 116 117 118 119 120 121 122 123 124 125 126 127 128 129 130 131 132 133 134 135 136 137 138 139 140 141 142 143 144 145 146 147 148 149 150 151 152 153 154 155 156 157 158 159 160 161 162 163 164 165 166 167 168 169 170 171 172 173 174 175 176 177 178 179 180 181 182 183 184 185 186 187 188 189 190 191 192 193 194 195 196 197 198 199 200 201 202 203 204 205 206 207 208 209 210 211 212 213 214 215 216 217 218 219 220 221 222 223 224 225 226 227 228 229 230 231 232 233 234 235 236 237 238 239 240 241 242 243 244 245 246 247 248 249 250 251 252 253 254 255 256 257 258 259 260 261 262 263 264 265 266 267 268 269 270 271 272 273 274 275 276 277 278 279 280 281 282 283 284 285 286 287 288 289 290 291 292 293 294 295 296 297 298 299 300 301 302 303 304 305 306 307 308 309 310 311 312 313 314 315 316 317 318 319 320 321 322 323 324 325 326 327 328 329 330 331 332 333 334 335 336 337 338 339 340 341 342 343 344 345 346 347 348 349 350 351 352 353 354 355 356 357 358 359 360 361 362 363 364 365 366 367 368 369 370 371 372 373 374 375 376 377 378 379 380 381 382 383 384 385 386 387 388 389 390 391 392 393 394 395 396 397 398 399 400 401 402 403 404 405 406 407 408 409 410 411 412 413 414 415 416 417 418 419 420 421 422 423 424 425 426 427 428 429 430 431 432 433 434 435 436 437 438 439 440 441 442 443 444 445 446 447 448 449 450 451 452 453 454 455 456 457 458 459 460 461 462 463 464 465 466 467 468 469 470 471 472 473 474 475 476 477 478 479 480 481 482 483 484 485 486 487 488 489 490 491 492 493 494 495 496 497 498 499 500 501 502 503 504 505 506 507 508 509 510 511 512 513 514 515 516 517 518 519 520 521 522 523 524 525 526 527 528 529 530 531 532 533 534 535 536 537 538 539 540 541 542 543 544 545 546 547 548 549 550 551 552 553 554 555 556 557 558 559 560 561 562 563 564 565 566 567 568 569 570 571 572 573 574 575 576 577 578 579 580 581 582 583 584 585 586 587 588 589 590 591 592 593 594 595 596 597 598 599 600 601 602 603 604 605 606 607 608 609 610 611 612 613 614 615 616 617 618 619 620 621 622 623 624 625 626 627 628 629 630 631 632 633 634 635 636 637 638 639 640 641 642 643 644 645 646 647 648 649 650 651 652 653 654 655 656 657 658 659 660 661 662 663 664 665 666 667 668 669 670 671 672 673 674 675 676 677 678 679 680 681 682 683 684 685 686 687 688 689 690 691 692 693 694 695 696 697 698 699 700 701 702 703 704 705 706 707 708 709 710 711 712 713 714 715 716 717 718 719 720 721 722 723 724 725 726 727 728 729 730 731 732 733 734 735 736 737 738 739 740 741 742 743 744 745 746 747 748 749 750 751 752 753 754 755 756 757 758 759 760 761 762 763 764 765 766 767 768 769 770 771 772 773 774 775 776 777 778 779 780 781 782 783 784 785 786 787 788 789 790 791 792 793 794 795 796 797 798 799 800 801 802 803 804 805 806 807 808 809 810 811 812 813 814 815 816 817 818 819 820 821 822 823 824 825 826 827 828 829 830 831 832 833 834 835 836 837 838 839 840 841 842 843 844 845 846 847 848 849 850 851 852 853 854 855 856 857 858 859 860 861 862 863 864 865 866 867 868 869 870 871 872 873 874 875 876 877 878 879 880 881 882 883 884 885 886 887 888 889 890 891 892 893 894 895 896 897 898 899 900 901 902 903 904 905 906 907 908 909 910 911 912 913 914 915 916 917 918 919 920 921 922 923 924 925 926 927 928 929 930 931 932 933 934 935 936 937 938 939 940 941 942 943 944 945 946 947 948 949 950 951 952 953 954 955 956 957 958 959 960 961 962 963 964 965 966 967 968 969 970 971 972 973 974 975 976 977 978 979 980 981 982 983 984 985 986 987 988 989 990 991 992 993 994 995 996 997 998 999 1000	16. DISTRIBUTION STATEMENT (of this Report)  Approved for public release; distribution unlimited
17. DISTRIBUTION STATEMENT (of the abstract entered in Block 20, if different from Report)  N/A			
18. SUPPLEMENTARY NOTES			
19. KEY WORDS (Continue on reverse side if necessary and identify by block number)  Acoustical disturbances Boundary layer Transition Stability			
20. ABSTRACT (Continue on reverse side if necessary and identify by block number)  The analysis of transition from laminar to turbulent flow on a flat plate has been the subject of numerous investigations. In the present work, emphasis has been placed on establishing a computational technique which can be utilized to develop a basic understanding of the effects of the propagation of acoustic waves into a boundary layer, and the ultimate effect of such disturbances on transition. The nonlinear system of unsteady compressible partial differential equations have been solved by a MacCormack predictor-corrector scheme which allows the effects of imposed disturbances to be tracked in time. The question			

DD FORM 1 JAN 73 1473

EDITION OF 1 NOV 65 IS OBSOLETE

Unclassified

SECURITY CLASSIFICATION OF THIS PAGE (When Data Entered)

409 964



Unclassified

SECURITY CLASSIFICATION OF THIS PAGE(When Data Entered)

of the mismatch in propagation velocity between Tollmein Schlichting and acoustic waves has been studied. The program indicates that while disturbances are propagating with the speed of sound in the inviscid flow, the waves well within the boundary layer are propagating at a speed on the order of the freestream velocity and thus the boundary layer is being excited by the classical Tollmein Schlichting waves. The analysis thus indicates that the effect of acoustical disturbances on transition is similar to the effect of other perturbations as experiments have indicated. 7

SECURITY CLASSIFICATION OF THIS PAGE(When Data Entered)

#### ACKNOWLEDGEMENT

This technical report covers the work performed under Contract N00014-76-C-1083 from 15 September 1975 to 15 December 1977 and is the annual report for this period. The program is sponsored by the Office of Naval Research.

ACCESSION for	
NTIS	Write Section <input checked="" type="checkbox"/>
DDC	Buff Section <input type="checkbox"/>
UNANNOUNCED	<input type="checkbox"/>
JUL 1 1978	
BY	
DISTRIBUTION/AVAILABILITY NOTES	
Dis:	ONE
A	

## TABLE OF CONTENTS

	Page
I. INTRODUCTION	1
II. METHOD OF ANALYSIS	4
A. Equations of Motion	4
B. Initial and Boundary Conditions	7
C. Numerical Method	12
III. THE PRESENT INVESTIGATION AND RESULTS TO DATE	15
IV. REFERENCES	30
DISTRIBUTION LIST	

## I. INTRODUCTION

In recent years several investigators (for example, Refs. 1 and 2) have developed numerical analyses to investigate the nonlinear effects of disturbances propagating in a laminar boundary layer with a view towards a better understanding of boundary layer stability. Such investigations are extensions of earlier linear stability analyses (for example, Refs. 3-7) and were motivated by the work of Stuart<sup>8</sup> and others who viewed the transition process as a series of distinctly observable stages. In the first stage, the two dimensional Tollmien-Schlichting waves are developed and the flowfield can be analyzed linearly. However, downstream of this region, nonlinear and three dimensional effects begin to play a more and more dominant role. Thus a complete physical understanding of the transition phenomenon must await the development of a nonlinear, three dimensional program capable of measuring amplification of the waves as they propagate.

Numerical analyses capable of solving the nonlinear system of equations in the boundary layer (even two dimensional codes) can be extremely useful for the study of the wave amplification phenomenon. Linear stability theory, exemplified by eigen solutions of the Orr-Sommerfeld equations, cannot directly incorporate the properties of imposed disturbances. Once disturbances are introduced, the mechanism of introduction not appearing in these solutions, it is presumed that they can no longer significantly influence the boundary layer process, which is, perhaps, a serious shortcoming of linear theory.

Nonlinear analyses (such as Refs. 1 and 2) have investigated the stability of laminar, incompressible boundary layers and the initial phase of the transition process (prior to the three dimensional bursting phase) by direct numerical solution of the partial differential equations which describe such a process. The boundary layer flow on a flat plate is disturbed by forced time-dependent



perturbations, and the reaction of the flow, i.e. the temporal and spatial development of the perturbations, is determined by a numerical solution of the governing equations. Such programs thus have the ability to analyze the effects of large scale disturbances (i.e. on the order of .1% of the free stream velocity) and how they are amplified or damped by the boundary layer, whereas linear stability programs cannot directly incorporate the effect of disturbance amplitude into the stability calculation.

While these nonlinear analyses represent a significant advance in the state of the art, they are restricted to incompressible flow. The effects of such parameters as Mach number and wall temperature are, of course, of great significance and a compressible analog to these methods is necessary.

In addition, such programs are unable to determine directly the effects of imposed acoustical disturbances. Experiments, for example Refs. 9 and 10, have indicated that the effects of imposed acoustic perturbations on boundary layer transition is similar to the effects of freestream turbulence<sup>11</sup> in low speed flow. One would expect waves propagating through the flowfield at the speed of sound to affect boundary layer transition in a different way than waves propagating through at the freestream velocity, but the Spangler and Wells experiments, as well as others, have shown that this is not the case. The frequency range which affects transition at a given Reynolds number is the same as when freestream disturbances are introduced, even though there appears to be a mismatch in propagation velocity (and thus in wave number).

The necessity for a study of the effects of these acoustical disturbances was the motivation of the present investigation and it's extension. The unsteady, compressible, second order boundary layer equations have been utilized. Terms of the order of the reciprocal of the Reynolds number and the reciprocal squared have been retained and thus the system is consistent with the Navier Stokes equations. These equations have been solved by an

explicit scheme in the high Reynolds number range (where the equations are, essentially, the boundary layer equations) consistent with the experiments of Spangler and Wells.

In Section II, the equations of motion and, method of analysis is developed. In Section III, the results and conclusions of the present investigation are presented. This work is part of a continuing effort and additional results, especially with regards to the effects of such parameters as Mach number and wall temperature, will be forthcoming.

## II. METHOD OF ANALYSIS

### A. Equations of Motion

The system of equations have have been utilized are the compressible, two-dimensional, higher order boundary layer equations (retaining terms of order  $1/Re$  and  $1/Re^2$ ). This system is thus, essentially, the compressible Navier Stokes equations. For unit Prandtl number, the system, for a perfect gas is;

$$\frac{\partial \bar{\rho}}{\partial \bar{t}} + \frac{\partial}{\partial \bar{x}} (\bar{\rho} \bar{u}) + \frac{\partial}{\partial \bar{y}} (\bar{\rho} \bar{v}) = 0 \quad (1)$$

$$\frac{\partial}{\partial \bar{t}} (\bar{\rho} \bar{u}) + \frac{\partial}{\partial \bar{x}} (\bar{\rho} \bar{u}^2 + \bar{p}) + \frac{\partial}{\partial \bar{y}} (\bar{\rho} \bar{u} \bar{v}) = \frac{\partial}{\partial \bar{y}} \left[ \bar{\mu} \frac{\partial \bar{u}}{\partial \bar{y}} \right] + \phi_1$$

$$\frac{\partial}{\partial \bar{t}} (\bar{\rho} \bar{v}) + \frac{\partial}{\partial \bar{x}} (\bar{\rho} \bar{u} \bar{v}) + \frac{\partial}{\partial \bar{y}} \left[ \bar{\rho} \bar{v}^2 + Re_L \cdot \bar{p} \right] = \frac{4}{3} \frac{\partial}{\partial \bar{y}} \left[ \bar{\mu} \frac{\partial \bar{v}}{\partial \bar{y}} \right] \quad (2)$$

$$- \frac{2}{3} \frac{\partial}{\partial \bar{y}} \left( \bar{\mu} \frac{\partial \bar{u}}{\partial \bar{x}} \right) + \frac{\partial}{\partial \bar{x}} \left( \bar{\mu} \frac{\partial \bar{u}}{\partial \bar{y}} \right) + \phi_2 \quad (3)$$

$$\frac{\partial}{\partial \bar{t}} (\bar{\rho} \bar{E}) + \frac{\partial}{\partial \bar{x}} (\bar{\rho} \bar{u} \bar{H}) + \frac{\partial}{\partial \bar{y}} (\bar{\rho} \bar{v} \bar{H}) = \frac{\partial}{\partial \bar{y}} \left[ \bar{\mu} \frac{\partial \bar{H}}{\partial \bar{y}} \right] + \phi_3 \quad (4)$$

$$\bar{p} = \bar{\rho} \cdot \bar{T} \quad (5)$$

where

$$\bar{x} = \frac{x}{L}; \quad \bar{y} = \frac{y}{L} \cdot \sqrt{Re_L}; \quad \bar{t} = t \frac{u_\infty}{L}$$

$$\bar{u} = \frac{u}{u_\infty}; \quad \bar{v} = \frac{v}{u_\infty} \cdot \sqrt{Re_L}; \quad \bar{p} = \frac{p}{\rho_\infty u_\infty^2}; \quad \bar{\rho} = \frac{\rho}{\rho_\infty}$$

$$\bar{H} = \frac{H}{u_\infty^2} = \frac{C_p T}{u_\infty^2} + \frac{u^2 + v^2}{2u_\infty^2}; \quad \bar{E} = \frac{E}{u_\infty^2} = \frac{C_v T}{u_\infty^2} + \frac{u^2 + v^2}{2u_\infty^2}$$

$$\bar{\mu} = \frac{\mu}{\mu_\infty} = \frac{T_\infty + 198.6}{T + 198.6} \left( \frac{T}{T_\infty} \right)^{3/2}; \quad \bar{T} = \frac{RT}{u_\infty^2} \quad Re_L = \frac{\rho_\infty u_\infty L}{\mu_\infty}$$

$$\phi_1 = \frac{1}{Re_L} \left[ \frac{4}{3} \frac{\partial}{\partial \bar{x}} \left( \bar{\mu} \frac{\partial \bar{u}}{\partial \bar{x}} \right) - \frac{2}{3} \frac{\partial}{\partial \bar{x}} \left( \bar{\mu} \frac{\partial \bar{v}}{\partial \bar{y}} \right) + \frac{\partial}{\partial \bar{y}} \left( \bar{\mu} \frac{\partial \bar{v}}{\partial \bar{x}} \right) \right]$$

$$\phi_2 = \frac{1}{Re_L} \frac{\partial}{\partial \bar{x}} \left( \bar{\mu} \frac{\partial \bar{v}}{\partial \bar{x}} \right)$$

$$\begin{aligned} \phi_3 = & \frac{1}{Re_L} \left[ \frac{\partial}{\partial \bar{x}} \left( \bar{\mu} \frac{\partial \bar{H}}{\partial \bar{x}} \right) + \frac{1}{3} \bar{\mu} \left( \frac{\partial \bar{u}}{\partial \bar{x}} \right)^2 + \frac{1}{3} \bar{\mu} \left( \frac{\partial \bar{v}}{\partial \bar{y}} \right)^2 - \frac{2}{3} \bar{\mu} \frac{\partial \bar{u}}{\partial \bar{x}} \frac{\partial \bar{v}}{\partial \bar{y}} + 2 \bar{\mu} \frac{\partial \bar{v}}{\partial \bar{x}} \frac{\partial \bar{u}}{\partial \bar{y}} \right. \\ & - \frac{1}{2} \frac{\partial \bar{\mu}}{\partial \bar{x}} \frac{\partial}{\partial \bar{x}} (\bar{u}^2) - \frac{1}{2} \frac{\partial \bar{\mu}}{\partial \bar{x}} \frac{\partial \bar{v}^2}{\partial \bar{x}} \frac{1}{Re_L} - \frac{1}{2} \frac{\partial \bar{\mu}}{\partial \bar{y}} \frac{\partial \bar{v}^2}{\partial \bar{y}} \left. \right] \\ & - \frac{1}{2} \frac{\partial \bar{\mu}}{\partial \bar{y}} \frac{\partial \bar{u}^2}{\partial \bar{y}} \end{aligned}$$

In order to study the effect of the propagation of acoustical free-stream disturbances, the equations have been transformed by a stretched coordinate system which packs many points into the boundary layer, but allows for a significant distribution of data in the freestream. The transformation utilized is:

$$\eta = 1 - \exp(-\alpha \bar{y} / \bar{\delta}^*) \quad (6)$$

where  $\bar{\delta}^* = \delta_0^* / L \sqrt{Re_L}$  and  $\delta_0^*(x)$  is the initial boundary layer displacement thickness distribution (i.e., the distribution at  $\bar{t} = 0$ ). Thus by varying  $\alpha$  one can pack as many points as needed near the surface (note as  $\bar{y} \rightarrow \infty, \eta \rightarrow 1$ ).

The system of equations in the transformed system is;

$$\frac{\partial \bar{\rho}}{\partial \bar{t}} + \frac{\partial}{\partial \bar{x}} (\bar{\rho} \bar{u}) + \frac{\partial}{\partial \eta} (\bar{\rho} \bar{u}) \frac{\partial \eta}{\partial \bar{x}} + (1 - \eta) \frac{\alpha}{\bar{\delta}^*} \frac{\partial \bar{\rho} \bar{v}}{\partial \eta} = 0 \quad (7)$$

$$\begin{aligned} & \frac{\partial}{\partial \bar{t}} (\bar{\rho} \bar{u}) + \frac{\partial}{\partial \bar{x}} (\bar{\rho} \bar{u}^2) + \bar{p} + \frac{\partial}{\partial \eta} (\bar{\rho} \bar{u}^2 + \bar{p}) \frac{\partial \eta}{\partial \bar{x}} + (1 - \eta) \frac{\alpha}{\bar{\delta}^*} \frac{\partial}{\partial \eta} (\bar{\rho} \bar{u} \bar{v}) \\ & = \frac{\alpha^2 (1 - \eta)}{\bar{\delta}^{*2}} \frac{\partial}{\partial \eta} [\bar{\mu} (1 - \eta) \frac{\partial \bar{u}}{\partial \eta}] + \phi_4 \end{aligned} \quad (8)$$



$$\frac{\partial}{\partial t} (\bar{\rho}\bar{v}) + \frac{\partial}{\partial x} (\bar{\rho}\bar{u}\bar{v}) + \frac{\partial}{\partial \eta} (\bar{\rho}\bar{u}\bar{v}) \frac{\partial \eta}{\partial x} - (1 - \eta) \frac{\alpha}{\delta^*} \frac{\partial}{\partial \eta} (\bar{\rho}\bar{v}^2 + \bar{p} \text{Re}_L) \quad (9)$$

$$= \frac{4}{3} \frac{\alpha^2}{\delta^{*2}} (1 - \eta) \frac{\partial}{\partial \eta} [\bar{\mu}(1 - \eta) \frac{\partial \bar{v}}{\partial \eta}] - \frac{2}{3} (1 - \eta) \frac{\alpha}{\delta^*} \frac{\partial}{\partial \eta} [\bar{\mu} \frac{\partial \bar{u}}{\partial x} + \bar{\mu} \frac{\partial \eta}{\partial x} \frac{\partial \bar{u}}{\partial \eta}]$$

$$+ \frac{\partial}{\partial x} [\bar{\mu} (1 - \eta) \frac{\alpha}{\delta^*} \frac{\partial \bar{u}}{\partial \eta}] + \frac{\partial \eta}{\partial x} \frac{\partial}{\partial \eta} [\bar{\mu} (1 - \eta) \frac{\alpha}{\delta^*} \frac{\partial \bar{u}}{\partial \eta}] + \phi_5$$

$$\frac{\partial}{\partial t} (\bar{\rho}\bar{E}) + \frac{\partial}{\partial x} (\bar{\rho}\bar{u}\bar{H}) + \frac{\partial}{\partial \eta} (\bar{\rho}\bar{u}\bar{H}) \frac{\partial \eta}{\partial x} + (1 - \eta) \frac{\alpha}{\delta^*} \frac{\partial}{\partial \eta} (\bar{\rho}\bar{u}\bar{H}) \quad (10)$$

$$= \frac{\alpha^2 (1 - \eta)}{\delta^{*2}} \frac{\partial}{\partial \eta} [\bar{\mu}(1 - \eta) \frac{\partial \bar{H}}{\partial \eta}] + \phi_6$$

$$\bar{p} = \bar{\rho}\bar{T} \quad (11)$$

where

$$\phi_4 = \frac{1}{\text{Re}_L} \left\{ \frac{4}{3} \frac{\partial}{\partial x} (\bar{\mu} \frac{\partial \bar{u}}{\partial x}) - \frac{2}{3} \frac{\alpha}{\delta^*} \frac{\partial}{\partial x} [\bar{\mu} (1 - \eta) \frac{\partial \bar{v}}{\partial \eta}] \right.$$

$$+ \frac{4}{3} \frac{\partial \eta}{\partial x} \frac{\partial}{\partial \eta} (\bar{\mu} \frac{\partial \bar{u}}{\partial x}) - \frac{2}{3} \frac{\alpha}{\delta^*} \frac{\partial \eta}{\partial x} \frac{\partial}{\partial \eta} [\bar{\mu} (1 - \eta) \frac{\partial \bar{v}}{\partial \eta}]$$

$$+ (1 - \eta) \frac{\alpha}{\delta^*} \frac{\partial}{\partial \eta} (\bar{\mu} \frac{\partial \bar{v}}{\partial x})$$

$$+ \frac{4}{3} \frac{\partial}{\partial x} (\bar{\mu} \frac{\partial \eta}{\partial x} \frac{\partial \bar{u}}{\partial \eta}) + \frac{4}{3} \frac{\partial \eta}{\partial x} \frac{\partial}{\partial \eta} (\bar{\mu} \frac{\partial \eta}{\partial x} \frac{\partial \bar{u}}{\partial \eta})$$

$$\left. + \frac{\alpha}{\delta^*} (1 - \eta) \frac{\partial}{\partial \eta} (\bar{\mu} \frac{\partial \eta}{\partial x} \frac{\partial \bar{v}}{\partial \eta}) \right\}$$

$$\phi_5 = \frac{1}{\text{Re}_L} \left[ \frac{\partial}{\partial x} (\bar{\mu} \frac{\partial \bar{v}}{\partial x}) + \frac{\partial \eta}{\partial x} \frac{\partial}{\partial \eta} (\bar{\mu} \frac{\partial \bar{v}}{\partial x}) \right.$$

$$\left. + \frac{\partial}{\partial x} (\frac{\partial \eta}{\partial x} \frac{\partial \bar{v}}{\partial \eta}) + (\frac{\partial \eta}{\partial x}) \frac{\partial}{\partial \eta} (\frac{\partial \eta}{\partial x} \frac{\partial \bar{v}}{\partial \eta}) \right]$$

$$\phi_6 = \frac{1}{\text{Re}_L} \left\{ \left[ \frac{\partial}{\partial x} + \frac{\partial \eta}{\partial x} \frac{\partial}{\partial \eta} \right] [\bar{\mu} \frac{\partial \bar{H}}{\partial x} + \frac{\partial \eta}{\partial x} \frac{\partial \bar{H}}{\partial \eta}] \right.$$

$$+ \frac{1}{3} \bar{\mu} \left( \frac{\partial \bar{u}}{\partial x} + \frac{\partial \eta}{\partial x} \frac{\partial \bar{u}}{\partial \eta} \right)^2 + \frac{1}{3} \bar{\mu} \left( \frac{\partial \bar{v}}{\partial x} + \frac{\partial \eta}{\partial x} \frac{\partial \bar{v}}{\partial \eta} \right)^2$$

$$- \frac{2}{3} \frac{\alpha(1 - \eta)}{\delta^*} \bar{\mu} \left( \frac{\partial \bar{u}}{\partial x} + \frac{\partial \eta}{\partial x} \frac{\partial \bar{u}}{\partial \eta} \right) \frac{\partial \bar{v}}{\partial \eta}$$

$$+ \frac{2}{3} \frac{\alpha(1 - \eta)}{\delta^*} \bar{\mu} \left( \frac{\partial \bar{v}}{\partial x} + \frac{\partial \eta}{\partial x} \frac{\partial \bar{v}}{\partial \eta} \right) \frac{\partial \bar{u}}{\partial \eta}$$

$$\left. - \frac{1}{2} \left( \frac{\partial \bar{u}}{\partial x} + \frac{\partial \eta}{\partial x} \frac{\partial \bar{u}}{\partial \eta} \right) \left( \frac{\partial (\bar{u}^2)}{\partial x} + \frac{\partial \eta}{\partial x} \frac{\partial (\bar{u}^2)}{\partial \eta} \right) \right\}$$

$$\begin{aligned}
& - \frac{1}{2\text{Re}_L} \left( \frac{\partial \bar{u}}{\partial x} + \frac{\partial \eta}{\partial x} \frac{\partial \bar{u}}{\partial \eta} \right) \left( - \frac{\partial \bar{v}^2}{\partial x} + \frac{\partial \eta}{\partial x} \frac{\partial \bar{v}^2}{\partial \eta} \right) \\
& - \frac{1}{2} \frac{\alpha^2}{\delta^{*2}} (1 - \eta)^2 \frac{\partial \bar{v}^2}{\partial \eta} \} \\
& - \frac{\alpha^2}{\delta^{*2}} (1 - \eta)^2 \frac{\partial \bar{u}}{\partial \eta} \frac{\partial \bar{u}^2}{\partial \eta}
\end{aligned}$$

Equations (7) through (11) are the basic system of equations which have been numerically solved.

#### B. Initial and Boundary Conditions

The investigation has centered on a study of the amplification or damping of acoustical disturbances propagated into a boundary layer. The experiments of Spangler and Wells<sup>9</sup> who utilized an air-driven, rotating vane sound generator to create the disturbance without producing any appreciable turbulence, were used. Both the frequency and intensity of the sound source were varied experimentally. A low velocity boundary layer channel was run at a unit Reynolds number of  $2.4 \times 10^5/\text{ft.}$ , the channel wall representing the flat plate. Measurements of transition occurred at distances on the order of 10-20 feet, and thus the length Reynolds numbers of interest are in the  $10^6$  to  $10^7$  range (see next section).

In order to model this problem, a set of initial and boundary conditions must be established, consistent with the propagation of acoustical disturbances and at the same time consistent with the set of differential equations utilized. The initial data, consistent with equations (1) through (5) under steady state conditions, was originally established utilizing numerical techniques for subsonic boundary layer analysis with normal pressure gradients established by

the principal investigator and reported previously, i.e., Ref. 12. Thus the solution at  $\bar{t} = 0$  was the solution of the two dimensional steady boundary layer equations with normal momentum equation included.

During the past year, consistent with Refs. 1 and 2, the Blasius solution has been utilized (since for the cases of interest,  $M_\infty \approx .03$ ) and has caused no major problems.

At the wall ( $\eta = 0$ ), for a rigid body, one can neglect the effect of the wave on temperature, and for an adiabatic wall one can establish the following relations (if one drops terms of order  $1/Re$  which implies some inconsistency for lower  $Re$ )

$$\eta = 0 \quad (\bar{x} > \bar{x}^*)$$

$$\bar{u} = \bar{v} = \frac{\partial \bar{T}}{\partial \eta} = 0$$

$$\frac{\partial}{\partial \eta} (\ln \bar{p}) = \frac{\partial}{\partial \eta} [(\ln \bar{p})]_{\bar{t}} = 0 \quad \exp[-Re_L \int_0^{\bar{t}} \frac{\bar{p}}{\bar{\mu}} d\bar{t}]$$

$$\frac{\partial}{\partial \eta} (\ln \bar{p}) = \frac{\partial}{\partial \eta} [(\ln \bar{p})]_{\bar{t}} = 0 \quad \exp[-Re_L \int_0^{\bar{t}} \frac{\bar{p}}{\bar{\mu}} d\bar{t}]$$

The outer boundary condition ( $\eta \rightarrow 1$ ) is established by allowing the wave to travel as a plane wave with speed of sound  $c_\infty$ .

Much effort has been placed on the determination of a proper downstream boundary condition. It has been found, consistent with the results of Fasel<sup>1</sup>, that the boundary condition that yields the least upstream influence, and is thus superior to other possible ones (including a non reflective condition) is:

$$\frac{\partial^2 \bar{u}(\bar{x}_f, \bar{y}, \bar{t})}{\partial \bar{x}^2} = \bar{\alpha}^2 \bar{u}'$$

where  $\bar{\alpha} = fL/V_{ph}$  ( $f$  is the frequency and  $V_{ph}$  the phase velocity),  $\bar{u}'$  is the perturbation quantity ( $\bar{u} - \bar{u}_0$ ), and  $\bar{x}_f$  is the downstream boundary. This condition says that at the downstream boundary, the disturbance has a periodic form.



At  $\bar{t} = 0$ , an acoustical disturbance is initiated at  $\bar{x} \approx 0$  so that the velocity field at  $x = x^* \approx 0$  and  $\bar{t} > 0$  can be written as

$$\bar{u}(\bar{x}^*, \bar{y}, \bar{t}) = \bar{u}_0(\bar{x}^*, \bar{y}) + f_1(\bar{y}) \sin(\bar{\omega}\bar{t})$$

where  $\bar{u}_0(\bar{x}^*, \bar{y})$  is the velocity profile at  $\bar{t} = 0$ ,  $\bar{\omega} = 2\pi fL/U_\infty$  ( $f$  being the frequency of the imposed disturbance, in cycles per second) and  $f_1(\bar{y})$  is the disturbance profile near the leading edge. The form of  $f_1(\bar{y})$  has been the object of extensive analysis and is described here. The other boundary conditions at  $x = x^*$  are consistent with linear theory and are determined once the form of  $f_1(\bar{y})$  is known.

In order to derive appropriate perturbation profiles for use as the initial boundary condition in our program (at  $\bar{x} = \bar{x}^*$ ) the compressible analogue of the Orr-Sommerfeld equations must be solved. We have at present considered these equations in the inviscid limit and under the additional assumption of no temperature gradient in the mean flow.

Thus nondimensionalizing all lengths by the boundary layer thickness  $\delta$  at a suitable station along the plate, all velocities by the free stream speed of sound, and the pressure by  $\rho_\infty c_\infty^2$ , the linearized perturbation system solved is;

$$i(ku_0 - \omega)\rho + iku_0\rho + \frac{d}{dy}(\rho_0 V) = 0 \quad (12)$$

$$i(ku_0 - \omega)u + u'_0 V + \frac{ik}{\rho_0} p = 0 \quad (13)$$

$$i(ku_0 - \omega)V + \frac{1}{\rho_0} \frac{dp}{dy} = 0 \quad (14)$$

$$i(ku_0 - \omega)T + T'_0 V = i\left(\frac{\gamma - 1}{\rho_0}\right)(ku_0 - \omega)p \quad (15)$$

$$p/\rho_0 = \rho/\rho_0 + T/T_0 \quad (16)$$

where bars have been dropped and subscript zero refers to the profile at  $t = 0$ .

The appropriate boundary conditions are discussed below. As is customary the normal mode decomposition has been used, and hence we note that  $\rho, u, V, p, T$



are functions of  $y$ , the distance normal to the plate. The parameters  $\omega$  and  $k$ , the dimensionless frequency and wave number respectively are given by

$$\omega = \Omega \delta / c_{\infty}, \quad k = \bar{k} \delta$$

where  $\Omega$  and  $\bar{k}$  are dimensional quantities. The mean flow quantities

$$u_0 = M_{\infty} u_B \quad \text{and} \quad u'_0 = 5.6 \left( M_{\infty} \frac{du_B}{d\eta} \right)$$

are the dimensionless velocity and velocity gradient respectively where  $M_{\infty}$  is the freestream Mach number,  $u_B$  is the dimensionless Blasius profile and the factor 5.6 results from changing the normal coordinate from  $\eta$  to  $y$ .

Several simplifications can be made in equations (12 - 16). We have solved for  $p$ ,  $u$ ,  $v$  and  $T$  in terms of the pressure  $p$  and find that  $p$  must satisfy the second order equation

$$p'' - \frac{2ku'_0}{u_0 k - \omega} p' + \left[ \frac{(u_0 k - \omega)^2}{T_0} - k^2 \right] p = 0 \quad (17)$$

In solving this equation we have considered  $\omega$  as fixed and  $k$  as an unknown to be found. (In general, the phase velocity,  $V_p = \omega/k$  and the wave number can be complex). For the present we are considering neutral stability and thus  $k$  and  $V_p$  are real, however, we plan to extend the calculation to include complex  $k$ .

To derive suitable boundary conditions, we assume that at the plate the perturbation  $V$ , in the normal velocity is zero and since

$$V = \frac{i}{\rho_0 (ku_0 - \omega)} \frac{dp}{dy}$$

we take

$$\frac{dp}{dy} = 0 \quad \text{at} \quad y = 0.$$

To derive a boundary condition at the top of the boundary layer or in the free stream, we write equation (17) in the free stream, i.e. with  $u'_0 = 0$  and  $u_B = 1$ . Then the equation has constant coefficients and can be readily solved. The nature of the solutions, depends of course, on the sign of  $\lambda = - (M_{\infty} k - \omega)^2 + k^2$ .

For the frequency and Mach numbers considered,  $\lambda$  is positive and hence

$p = C_1 \exp(-\sqrt{\lambda}y)$  is the solution of (17) which vanishes at infinite distances from the plate. Using this solution to provide boundary conditions for the top of the boundary layer we have

$$\frac{dp(1)}{dy} = -\sqrt{\lambda} = -\sqrt{k^2 - (M_\infty^2 k - \omega)^2} \quad \text{and} \quad p(1) = 1 \quad (18)$$

We note that the second condition is a normalization condition.

Equations (12) - (17) now provide an eigenvalue problem for the eigenvalue  $k$ . Once  $k$  is determined, the profiles at  $x = \bar{x}^*$  (i.e. the  $f_1(y)$ ) can be determined and thus the initial and boundary conditions for the calculation are entirely prescribed.

### C. Numerical Method

The MacCormack predictor corrector scheme has been utilized in the study. Equations (7) - (10) are four equations of the form

$$\frac{\partial e}{\partial t} = a_1 \frac{\partial f}{\partial x} + a_2 \frac{\partial g}{\partial \eta} + a_3 \frac{\partial^2 h}{\partial \eta^2} + a_4 \frac{\partial^2 i}{\partial \bar{x}^2} + a_5 \frac{\partial^2 j}{\partial \bar{x} \partial \eta}$$

If these equations are written as

$$\frac{\partial e_i}{\partial t}(\bar{x}, \eta, \bar{t}) = F(\bar{x}, \eta, \bar{t})$$

$$e_1 = \bar{\rho}, \quad e_2 = \bar{\rho}u, \quad e_3 = \bar{\rho}v, \quad e_4 = \bar{\rho}\bar{E}$$

the MacCormack method states that

$$e(\bar{x}, \eta, \bar{t} + \Delta\bar{t}) = e(\bar{x}, \eta, \bar{t}) + 1/2[F(\bar{x}, \eta, \bar{t}) + F(\bar{x}, \eta, \bar{t} + \Delta\bar{t})]\Delta\bar{t}$$

In order to solve for  $e(\bar{x}, \eta, \bar{t} + \Delta\bar{t})$  one first calculates a provisional solution,

$$e^{(1)}(\bar{x}, \eta, \bar{t} + \Delta\bar{t}) = e(\bar{x}, \eta, \bar{t}) + F^{(+)}(\bar{x}, \eta, \bar{t}) \Delta\bar{t}$$

where  $F^{(+)}$  refers to evaluation by non-centered differences, using values at  $\bar{x} + \Delta\bar{x}$ ,  $\eta + \Delta\eta$ ,  $\bar{x}$ , and  $\eta$ , e. g.

$$\frac{\partial f}{\partial x} = \frac{f(\bar{x} + \Delta\bar{x}, \eta, \bar{t}) - f(\bar{x}, \eta, \bar{t})}{\Delta\bar{x}}$$

then one can use  $e^{(1)}$  to evaluate the term  $F^{(-)}(\bar{x}, \eta, \bar{t} + \Delta\bar{t})$  using non-centered differences based on  $\bar{x} - \Delta\bar{x}$ ,  $\eta - \Delta\eta$ ,  $\bar{x}, \eta$ ; e.g.,

$$\frac{\partial f}{\partial x} = \frac{f^{(-)}(\bar{x}, \eta, \bar{t} + \Delta\bar{t}) - f^{(-)}(\bar{x} - \Delta\bar{x}, \eta, \bar{t} + \Delta\bar{t})}{\Delta\bar{x}}$$

Thus one can solve for  $e(\bar{x}, \eta, \bar{t} + \Delta\bar{t})$  from the system,

$$e(\bar{x}, \eta, \bar{t} + \Delta\bar{t}) = 1/2[e(\bar{x}, \eta, \bar{t}) + e^{(1)}(\bar{x}, \eta, \bar{t} + \Delta\bar{t}) + F^{(-)}(\bar{x}, \eta, \bar{t} + \Delta\bar{t}) \Delta\bar{t}]$$



Equations (7) - (10), the full unsteady compressible Navier Stokes system are a complex set of elliptic differential equations to numerically integrate. No other nonlinear analysis, that we are aware of, has attempted to solve the compressible system for the present application (both Fasel and Murdock solve the incompressible problem). The explicit MacCormack scheme was seen as a simpler method for the solution of this system as opposed to an implicit (or ADI) method.

The problem with utilizing an explicit scheme for such calculations is manifested in the problem of the time step which can be utilized in order to insure a stable solution. Since  $\Delta y \ll \Delta x$  in the boundary layer, the time step to satisfy the C.F.L. condition is such that  $\Delta t < \Delta y/c$ , which is extremely small, and in order to insure on the order of ten time periods for the frequencies of interest, on the order of  $10^5$  time steps would be required. We have noticed though that for the problems of interest (the modeling of the experiments of Ref. 9) the local Reynolds numbers of interest are greater than  $10^6$  and thus the leading terms are the parabolic system (i.e., the first order boundary layer equations). The parabolic system has a much less stringent time size criteria (like  $\Delta t < \Delta y^2/2\nu$ ).

For the grid sizes used in the present investigation,  $\Delta \bar{t} \sim M_\infty \Delta \bar{x}$  satisfies the parabolic time step criteria ( $\Delta \bar{t} < \Delta y^2/2$ ). Over the time scale of interest (on the order of ten perturbation periods) the relaxation of the C.F.L. criteria is manifested not in a gross instability (because of the very high Reynolds numbers) but as a drift in the solution. This was noticed by imposing a zero perturbation field at the station  $\bar{x} = \bar{x}^*$  (i.e.,  $f_1(y) = 0$ ) and tracking the perturbation solution ( $\bar{u} - \bar{u}_{\text{Blasius}}$ ). The program was thus modified to circumvent this problem in the following manner. At any time step, the equations are solved under two sets of conditions, first for the flow without external disturbance (i.e.,  $f_1(y) = 0$ ) and then for the flow with disturbance. The solution of every point at each time step is then taken as



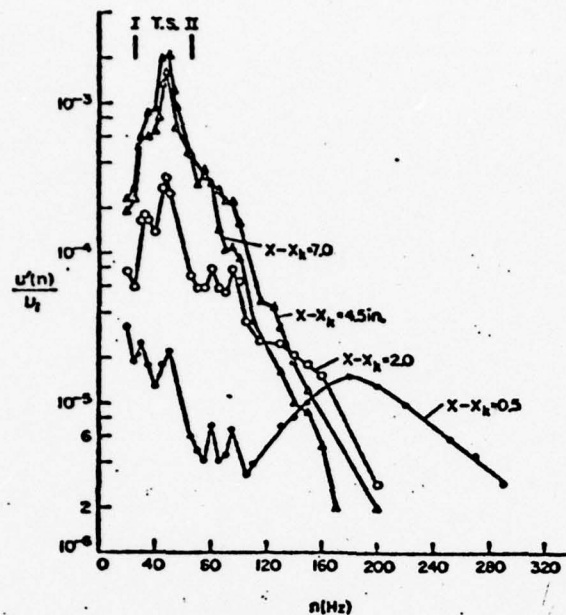
the difference between the two solutions. Thus it is felt that any errors due to numerics have been suppressed. The time traces which will be presented in the next section exhibit no drift and, thus, we feel that the oscillations at each position in the flowfield are due only to the disturbance imposed and are not numerical in nature. At lower Reynolds numbers or for times greater than those of the present calculations the error introduced by not satisfying the C.F.L. will grow and an instability will undoubtedly occur, necessitating one to resort to time splitting (or some other such technique). During the coming year, the program will be modified towards this end.

#### IV. THE PRESENT INVESTIGATION AND RESULTS TO DATE

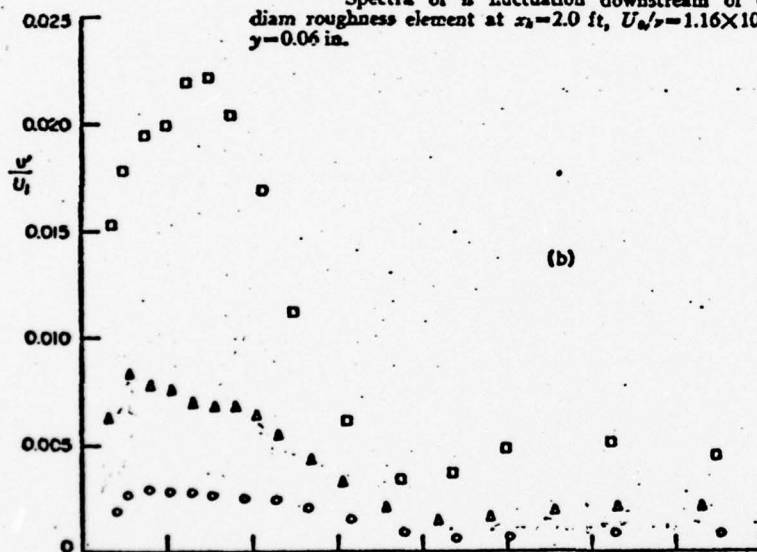
One of the tasks that was pursued this year was an attempt to interpret the results of experimental investigations of large scale (.1% to 1% of freestream) perturbations on boundary layer stability. The experimental results of Klebanoff and Tidstrom <sup>14</sup> for boundary layer transition induced by a two dimensional roughness element were examined in detail towards this end.

Figure 1 (reproduced from Reference 14) presents the longitudinal velocity fluctuations downstream of the roughness element. In the top figure, the fluctuations directly downstream of the element (located at  $x = x_k = 2$  ft) for a unit Reynolds number of  $1.16 \times 10^5/\text{ft}$  are plotted as a function of frequency. At the end of the recovery zone ( $x - x_k \approx 4.5$  in) amplification in the Tollmien Schlichting range has occurred. In the lower figure the transverse profiles, for a range of unit Reynolds numbers are presented. At larger unit Reynolds numbers, transition occurred in the recovery zone and the analysis presented below is no longer pertinent. For the unit Reynolds number  $1.16 \times 10^5/\text{ft}$  the boundary layer profile became highly inflected (and more unstable) downstream of the element until  $x - x_k = 4.5$  in where the profile returns to a Blasius representation, as is shown in Figure 2 taken from Reference 14. For this case, transition occurs at  $x - x_k = 19$  in.

Thus for a length of approximately two feet, a Blasius like flowfield is under the influence of a large perturbation ( $U'/U_\infty > .1\%$  at  $x - x_k = 4.5$  in) initial profile. This initial profile is shown by the triangles in (b) of the lower figure of Figure 1. This profile corresponds to a linear spatial stability profile for 50 cycles/sec (the dominant mode for the case) but for a somewhat higher Reynolds number (the roughness element has, of course, amplified the



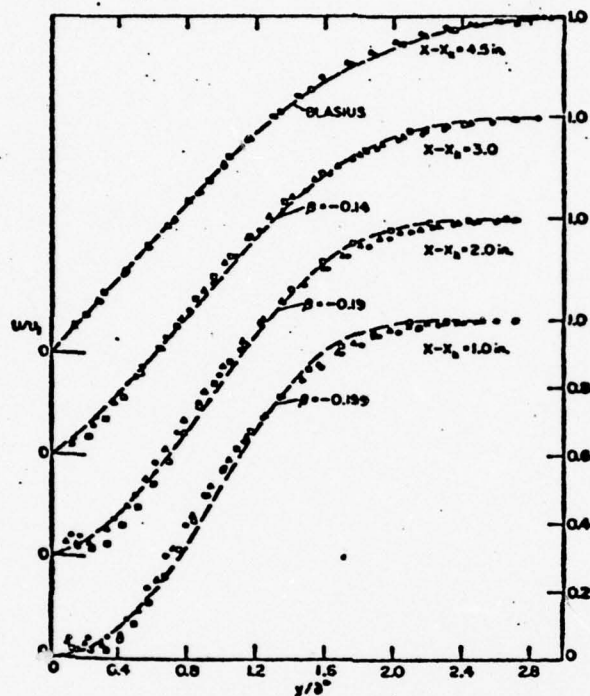
Spectra of  $u$  fluctuation downstream of 0.066-in. diam roughness element at  $x_2=2.0$  ft,  $U_0/v=1.16 \times 10^5$  ( $\text{ft}^{-1}$ ),  $y=0.06$  in.



Intensity of  $u$  fluctuation downstream of 0.066-in. diam roughness element at  $x_2=2.0$  ft, illustrating increase in amplification within recovery zone.  $\circ$   $U_0/v=1.0 \times 10^5$  ( $\text{ft}^{-1}$ ),  $\triangle$   $U_0/v=1.16 \times 10^5$  ( $\text{ft}^{-1}$ ),  $\square$   $U_0/v=1.42 \times 10^5$  ( $\text{ft}^{-1}$ ). (a)  $x-x_1=0.5$  in. (b)  $x-x_1=4.5$  in.



FIGURE 1. LONGITUDINAL VELOCITY FLUCTUATIONS DOWNSTREAM OF ROUGHNESS ELEMENT



Mean-velocity distributions downstream of 0.066-in. diam roughness element at  $x_1 = 2.0$  ft compared with Hartree profiles;  $\circ$   $U_0/\nu = 1.0 \times 10^5$  ( $\text{ft}^{-1}$ );  $\triangle$   $U_0/\nu = 1.16 \times 10^5$  ( $\text{ft}^{-1}$ );  $\square$   $U_0/\nu = 1.42 \times 10^5$  ( $\text{ft}^{-1}$ ).

FIGURE 2. MEAN PROFILES IN RECOVERY ZONE



the boundary layer response at this station). Therefore, downstream of  $x - x_k = 4.5$  in, the boundary layer is acting like a typical flat plate boundary layer under the influence of a large initial disturbance profile. We will attempt to show similarities between this flowfield (or the forced response to other larger scale perturbations) and the response to acoustical disturbances, by an examination of the results of our computer code.

For the computation of the acoustic response, one must first solve the linear acoustic stability problem (at  $\bar{x} = \bar{x}^*$ ) as described in the previous section. Such analyses have been performed. An eigenvalue search indicates that for a given frequency, the wave numbers corresponding to the eigen solutions occur at propagation velocities on the order of the freestream velocity (actually two to three times larger). Thus the results of Refs. 5 and 6 are correct, even for an acoustical disturbance, in the linear range.

The computer program for the solutions of equations (7) - (10) has been run for certain cases corresponding to the Reynolds number and frequency range of the Spangler and Wells experiments. Figure 3 presents the results of three such computations for the forced response of the boundary layer to acoustic waves of different frequencies (using linear stability theory at  $\bar{x}^* = .025$ ). For these cases the values of  $U'_{R.M.S.}$  taken was .3% of the freestream.

Linear stability theory would predict that for the length Reynolds number of interest for the Spangler and Wells experiments ( $\approx 3 \times 10^6$  at  $x = 12$  ft) a frequency of 27 cycles/sec is within the unstable region, whereas at 150 cycles/sec the flow is stable. This factor is evident in Figure 3. The 43 cycles/sec case exhibits neither amplification or damping (and thus appears neutrally stable) a factor which does not agree with the experimental results which show early transition at 43 cycles. It may be possible that if the computation were carried further in time some amplification would exist.

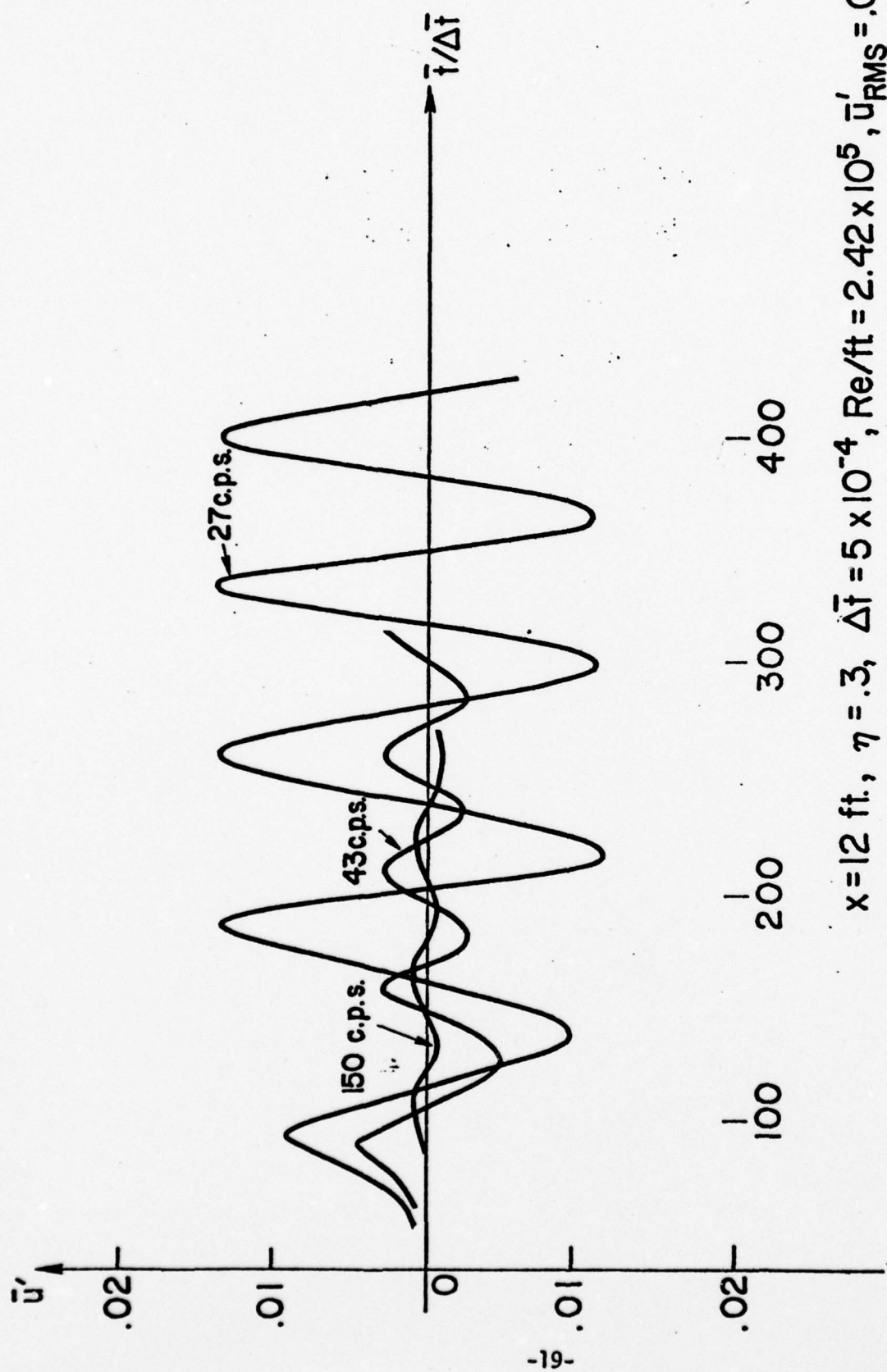


FIGURE 3. FREQUENCY DEPENDENCE ON DAMPING OR AMPLIFICATION OF ACOUSTICAL DISTURBANCE

Figures 4 and 5 present the temporal history, for the 27 cycle/sec case for  $U'_{R.M.S.} = .3\%$  of freestream at different stations downstream of the leading edge at two different transverse stations. As one moves significantly downstream (i.e., to  $x = 16$  ft) the level of amplification decreases (its maximum is at  $x = 8$  ft, corresponding to an  $Re_L = 1.9 \times 10^6$ ). Such results are in line with previous results, i.e., the amplification curves of Fasel<sup>1</sup> where the amplification increases as one passes into the instability region and decreases as the neutral stability curve is again crossed.

An illustration of severe damping is exhibited in Figure 6, which shows how a large perturbation is damped when the frequency is well outside of stability theory. The exceptionally high value of disturbance is almost completely damped at  $x = 6$  ft.

Much has been said about the effect of acoustics on transition, the application of linear stability theory with the mismatch of propagation velocities between turbulence and acoustic waves, and whether or not Tollmien Schlichting waves are excited under the influence of sound waves. Indeed, the frequency range of the experiments is in line with stability theory. An investigation was initiated to determine what the propagation speed inside the boundary layer was. In all cases, while the disturbances were propagating with the speed of sound along the freestream, the waves within the boundary layer were propagating at a speed of the order of the freestream speed, and thus indeed, the waves are the classical Tollmien Schlichting waves. Such a result is presented in Figure 7. This result is in agreement with the recent experiments reported in Ref. 10.

What is essentially occurring is that the wave propagating along the outer edge has little effect on the boundary layer development. Instead, the major effect is the profile at the leading edge, and thus, the effect of the acoustic wave is only to set up the initial disturbance field (i.e., at  $\bar{x} = \bar{x}^*$ ). Since



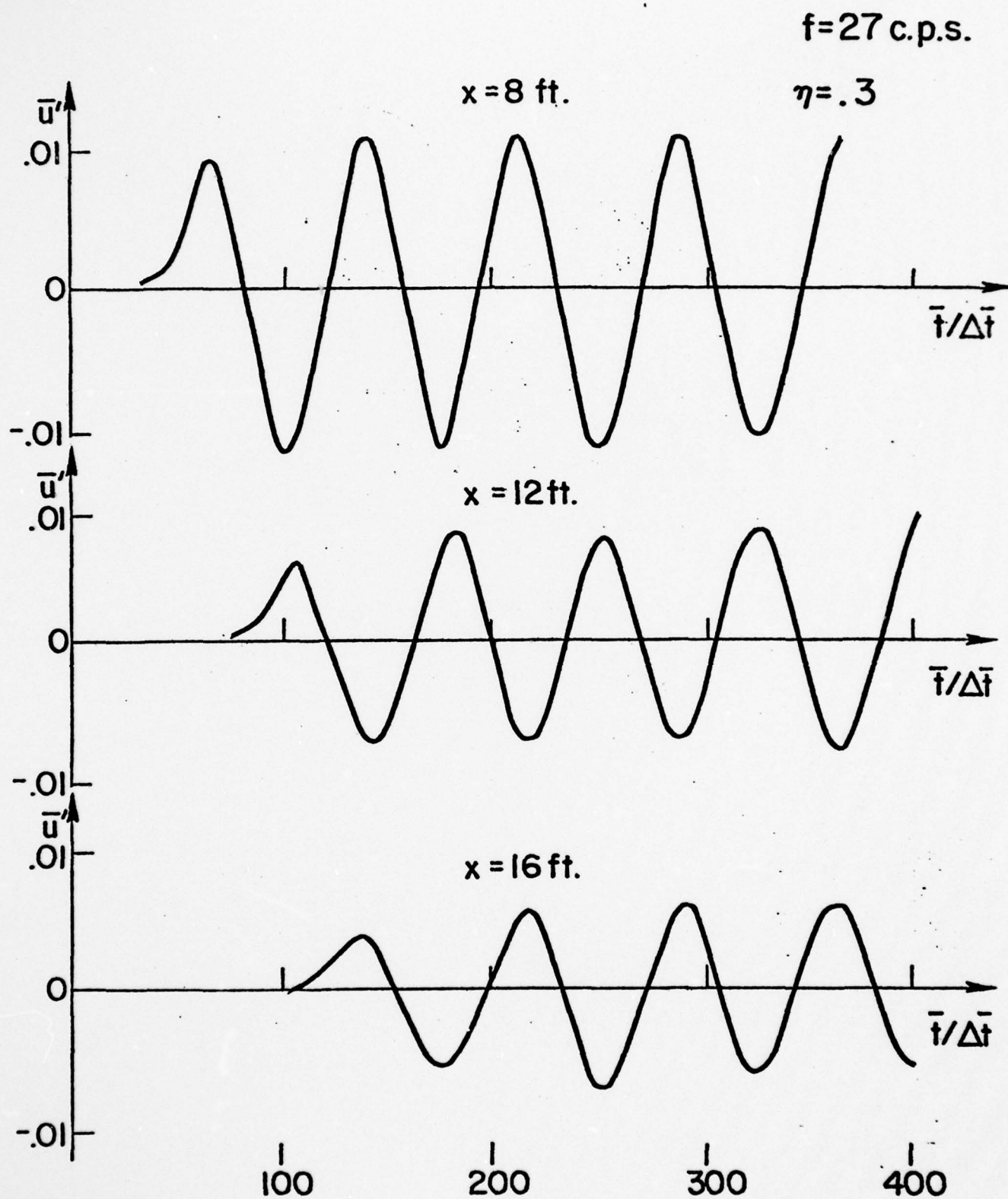


FIGURE 4. TEMPORAL HISTORY DOWNSTREAM OF IMPOSED DISTURBANCE ( $\eta = .3$ ,  $f = 27 \text{ cps}$ )

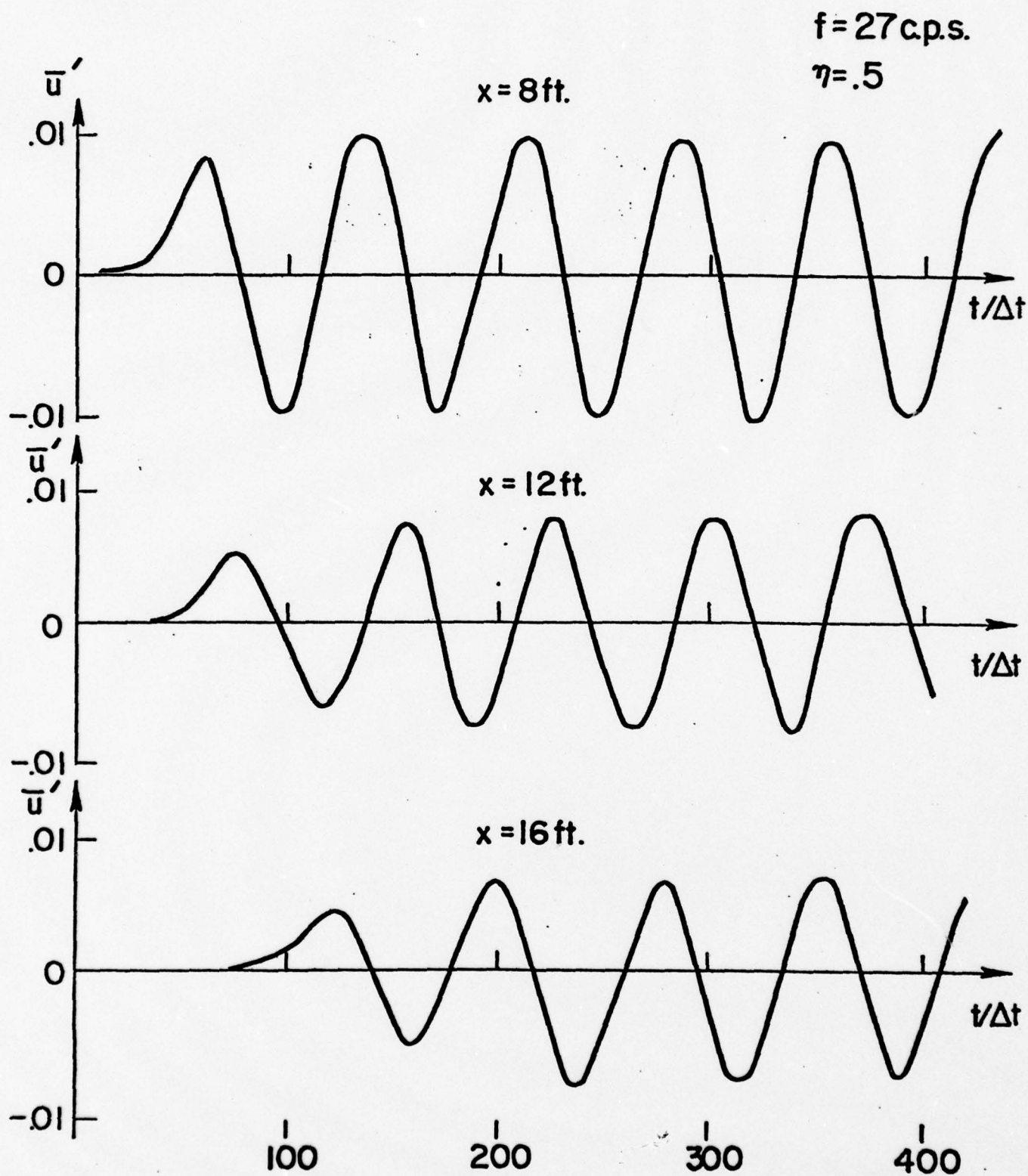


FIGURE 5: TEMPORAL HISTORY DOWNSTREAM OF IMPOSED DISTURBANCE ( $\eta = .5$ ,  $f = 27 \text{ cps}$ )

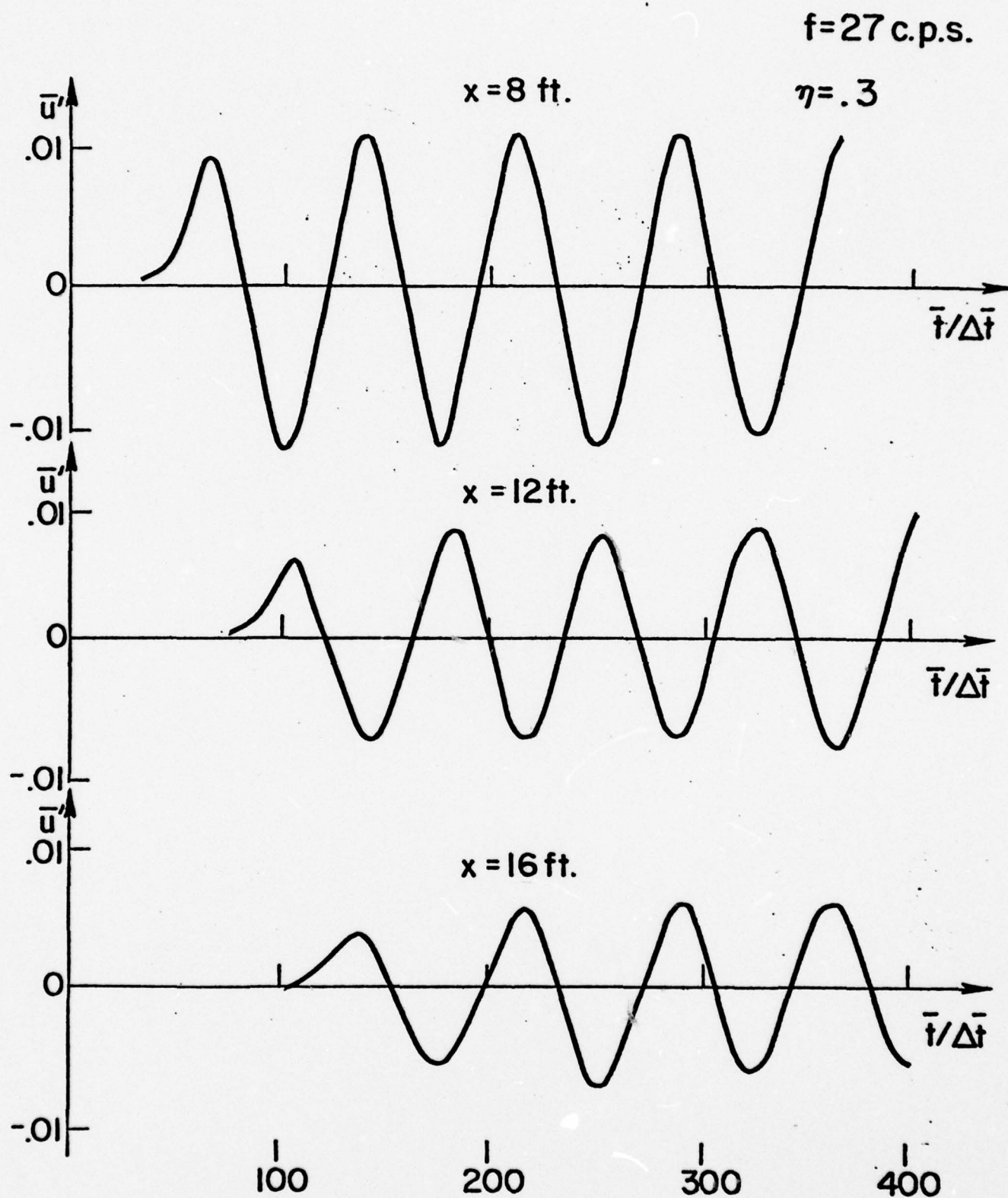


FIGURE 4. TEMPORAL HISTORY DOWNSTREAM OF IMPOSED DISTURBANCE ( $\eta = .3$ ,  $f = 27 \text{ cps}$ )



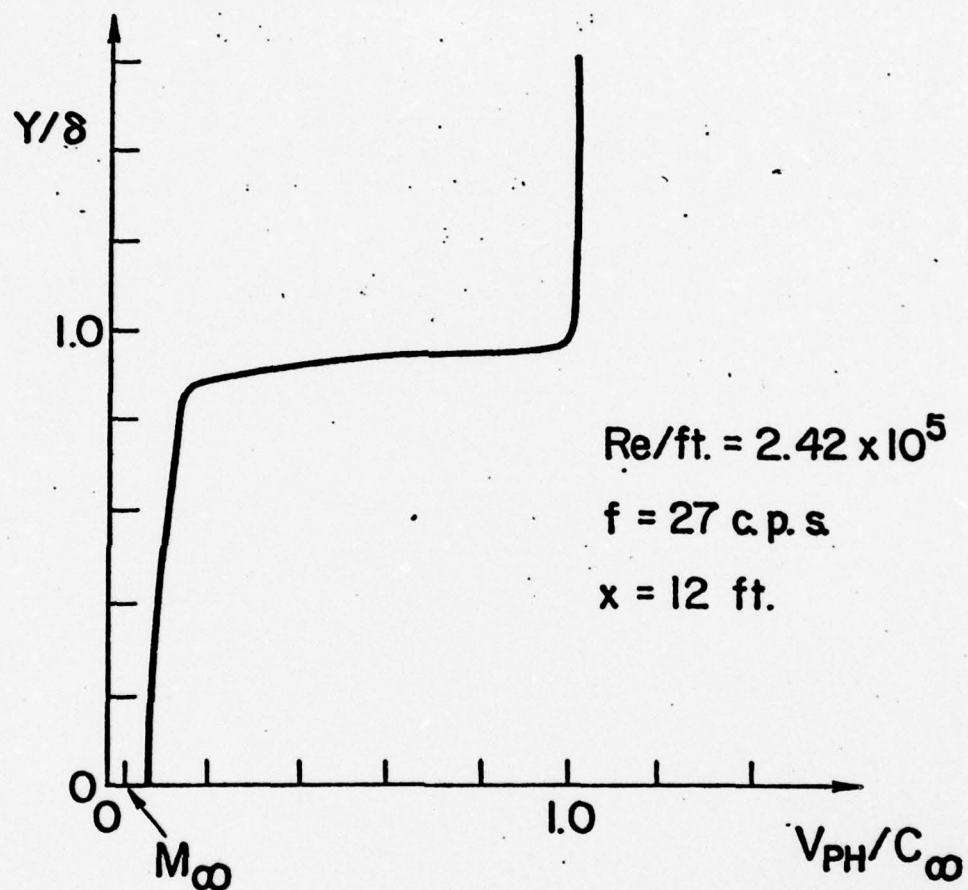


FIGURE 7. PHASE SPEED OF WAVES INSIDE BOUNDARY LAYER UNDER THE INFLUENCE OF ACOUSTICAL DISTURBANCE

we have found that the profiles of References 5 and 6 are representative of the acoustical disturbance profile near the leading edge, the effect of acoustics on transition is, indeed, similar to the effect of other large (or small) perturbations such as the roughness element effects described previously.

In order to test this result, a series of runs were made to compare the results of the present code to those of other investigations. Figures 8 and 9 illustrate how the results of the present analysis compare with the results of Ref. 2. Even though at the outer boundary, waves are propagating at a speed one to two orders of magnitude greater than the freestream velocity, the results of the present investigation with respect to boundary layer response are in good agreement with the results of Ref. 2.

Figure 10 illustrates a test case run to see how the method compares with linear stability theory. For the case  $U_\infty/\nu = .6 \times 10^5/\text{ft}$  and  $f = 25$  cps (with  $L = 12$  ft) linear stability theory predicts that the Reynolds number based on displacement thickness for neutral stability is approximately 1125. For  $Re^* < 1125$  waves are damped, for  $Re^* > 1125$  waves are amplified. The results of the present calculation indicate this to be the case, again confirming both the utility of the method and the fact that the response of a boundary layer to acoustic vibrations is similar to the response to other disturbance fields.

A remark is necessary with respect to the utility of the present analysis with respect to the problem of transition. There is much question as to the length of the three dimensional region prior to transition. Indeed, if three-dimensional effects predominate over a long distance prior to transition, two dimensional programs will be unable to predict transition accurately. Such a program though, can be of value with respect to determining basic flow structure in regions prior to the onset of transition, as has been demonstrated here.

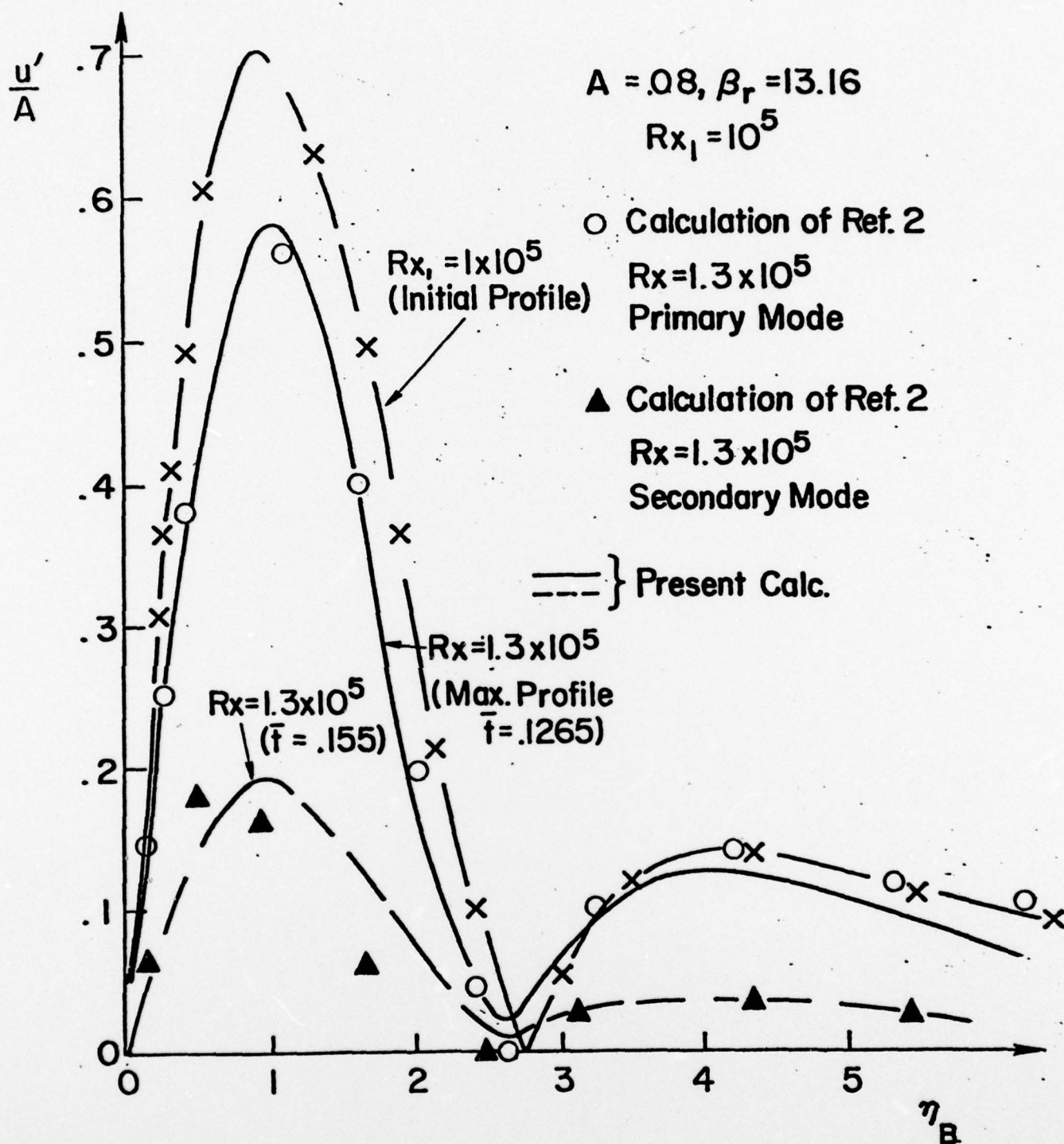


FIGURE 8. COMPARISON OF COMPUTED DISTURBANCE PROFILES WITH DATA OF REFERENCE 2



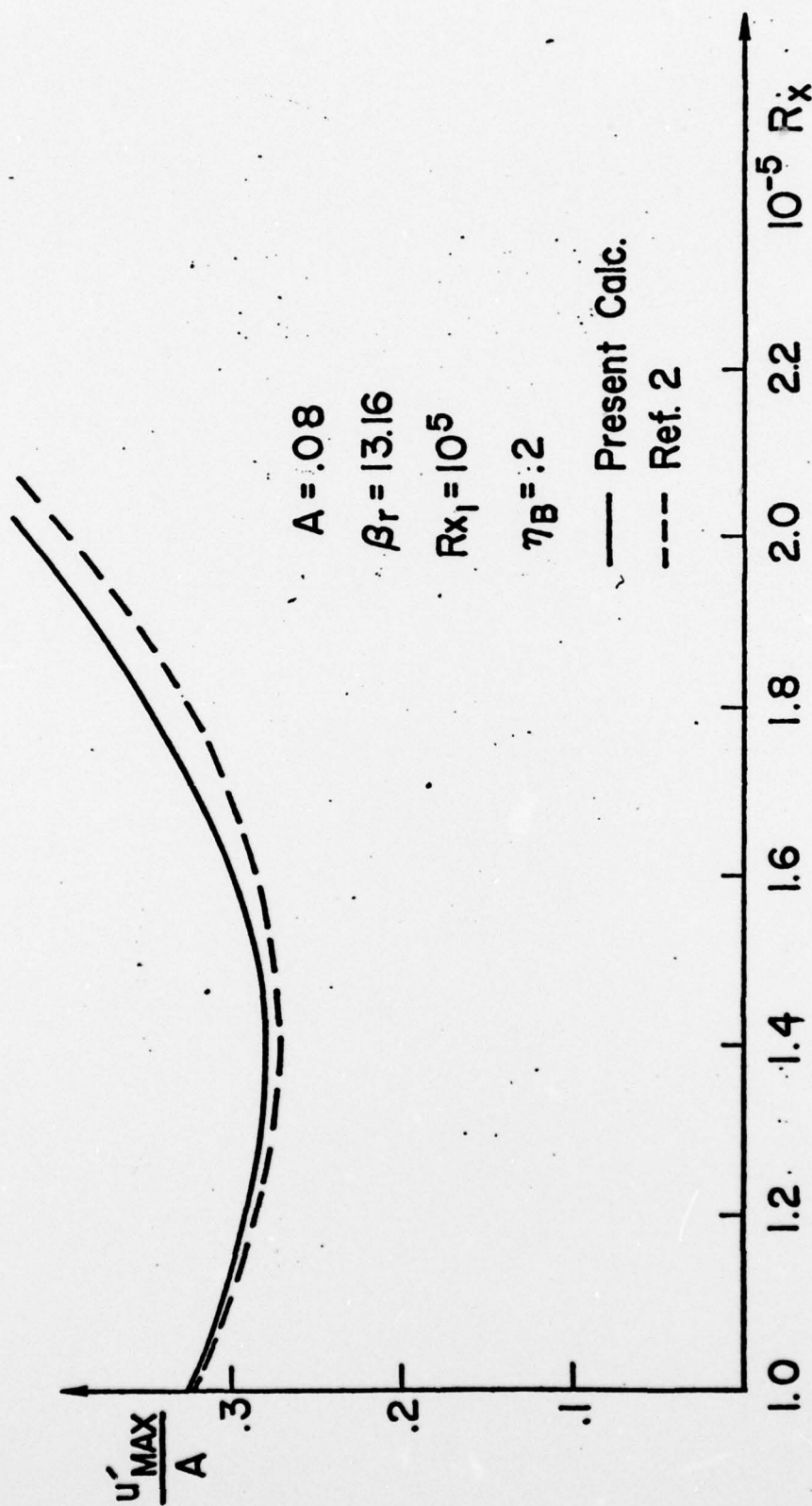


FIGURE 9. COMPARISON OF MAXIMUS DISTURBANCE DISTRIBUTION WITH DATA OF REFERENCE 2.

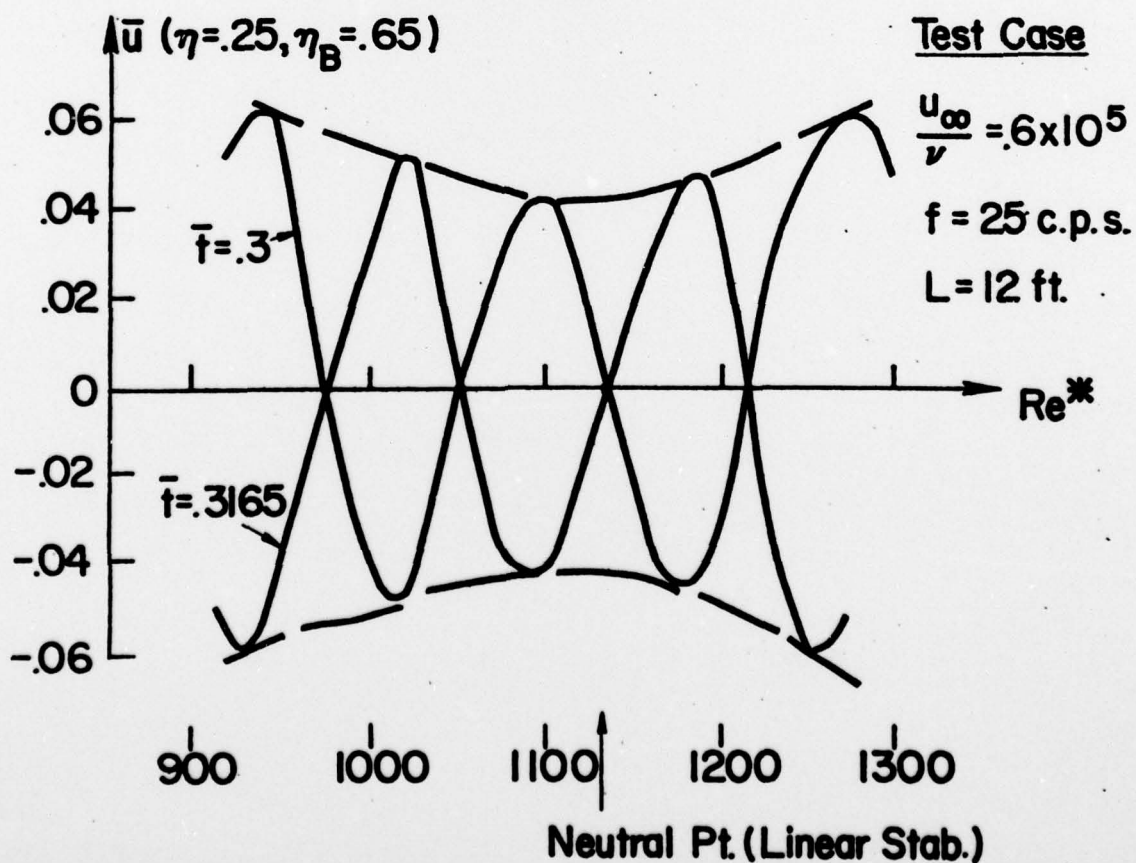
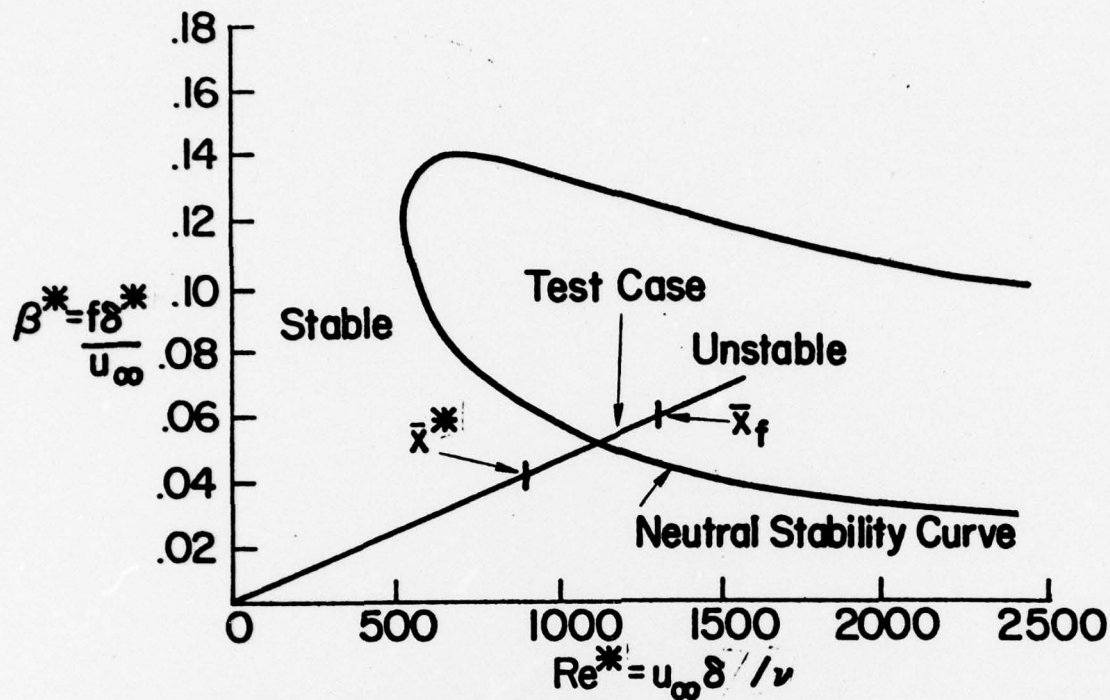


FIGURE 10. COMPARISON OF PROGRAM OUTPUT WITH LINEAR STABILITY THEORY

It is felt that the results achieved to date provide a fundamental understanding with respect to boundary layer response to acoustical disturbances. It seems necessary at this time that the numerical analysis and computer code be modified with respect to the marching step utilized in order to allow the program to have general applicability (for example, to allow the program to be utilized at lower Reynolds numbers). Therefore, in the coming year, the full, compressible, unsteady Navier Stokes equations will be reprogrammed and solved by an explicit MacCormack scheme with time splitting<sup>13</sup>. Thus the small time scale in the normal direction ( $\Delta t_y < \Delta y/c$ ) can be properly accounted for. There are advantages to utilizing an explicit scheme for the complex system to be solved (as opposed to a fully implicit scheme or an A.D.I.). When solving the full compressible Navier Stokes equations, all derivatives in x and y are immediately computed and thus the solution of the full system is no more complex, in principle, than the solution of the boundary layer system. In addition, whereas an implicit scheme allows one to utilize a bigger time step from a stability viewpoint one is still bound by the small time step criterion from the viewpoint of accuracy.

Once the program has been changed to allow for general applicability, the program will be extended so that a wide range of parameters can be varied. The effects of Mach number, type of disturbance, wall temperature, wall suction or injection, and wall compliance will be studied after the program has been properly modified.



#### IV. REFERENCES

1. Fasel, H., "Investigation of the Stability of Boundary Layers by a Finite Difference Model of the Navier Stokes Equations," *Journal of Fluid Mechanics*, Vol. 78, Part 2, 1976.
2. Murdock, J. W., "A Numerical Study of Nonlinear Effects on Boundary Layer Stability", *A.I.A.A.*, paper 77-127, January 1977.
3. Smith, A.M.O. and Gamberoni, N., "Transition, Pressure Gradient and Stability Theory," Douglas Aircraft Report ES-26388, 1956.
4. Mack, L.M., "*Computation of the Stability of the Laminar Compressible Boundary Layer*," *Methods in Computational Physics*, Vol. 4, B. Alder, ed., Academic Press, 1965.
5. Wazzan, A.R., Okamura, T.T. and Smith, A.M.O., "Space and Temporal Stability Charts," Douglas Aircraft Report DAC-67086, 1968.
6. Jordinson, R., "The Flat Plate Boundary Layer, Part 1. Numerical Integration of the Orr-Sommerfeld Equation", *Journal of Fluid Mechanics*, Vol. 43, Part 4, 1970.
7. Saric, W.S. and Nayfeh, A.H., "Nonparallel Stability of Boundary Layer Flows", *Journal of Physics of Fluids*, Vol. 18, No. 8, August 1975.
8. Stuart, J. T., "Hydrodynamic Stability," *Applied Mechanics Review*, Vol. 18, 1965.
9. Spangler, J.G. and Wells, C.S., "Effects of Freestream Disturbances on Boundary Layer Transition", *Journal of the American Institute of Aeronautics and Astronautics*, Vol. 6, No. 4, 1968.
10. Shapiro, P. J., "The Influence of Sound Upon Laminar Boundary Layer Stability", M.I.T. Rept. No. 83458-83560-1, September 1977.
11. Shubauer, G.B. and Skramstad, H.K., "Laminar Boundary Layer Oscillators and Transition on a Flat Plate", Report 909, NACA, 1948.
12. Miller, G. and Fanchiotti, "An Interaction Model for the Solution of Laminar Separation on a Surface", *A.I.A.A.* paper 75-5, January 1975.
13. McCormack, R.W., "The Effects of Viscosity in Hypervelocity Impact Cratering", *A.I.A.A.* paper 69-354, 1969.
14. Klebanoff, P.S. and Tidstrom, K.D., "Mechanism by Which a Two-Dimensional Roughness Element Induces Boundary Layer Transition", *Journal of Physics of Fluids*, Vol. 15, No. 7, 1972.



DISTRIBUTION LIST FOR UNCLASSIFIED  
TECHNICAL REPORTS AND REPRINTS ISSUED UNDER  
CONTRACT N00014-76-C-0183 TASK NR 061-232

All addresses receive one copy unless otherwise specified

Technical Library  
Building 313  
Ballistic Research Laboratories  
Aberdeen Proving Ground, MD 21005

Dr. F. D. Bennett  
External Ballistic Laboratory  
Ballistic Research Laboratories  
Aberdeen Proving Ground, MD 21005

Mr. C. C. Hudson  
Sandia Corporation  
Sandia Base  
Albuquerque, NM 81115

Professor P. J. Roache  
Ecodynamics Research  
Associates, Inc.  
P. O. Box 8172  
Albuquerque, NM 87108

Dr. J. D. Shreve, Jr.  
Sandia Corporation  
Sandia Base  
Albuquerque, NM 81115

Defense Documentation Center  
Cameron Station, Building 5  
Alexandria, VA 22314 12 Copies

Library  
Naval Academy  
Annapolis, MD 21402

Dr. G. H. Heilmeyer  
Director, Defense Advanced  
Research Projects Agency  
1400 Wilson Boulevard  
Arlington, VA 22209

Mr. R. A. Moore  
Deputy Director, Tactical  
Technology Office  
Defense Advanced Research Projects  
Agency  
1400 Wilson Boulevard  
Arlington, VA 22209

Office of Naval Research  
Code 411  
Arlington, VA 22217

Office of Naval Research  
Code 421  
Arlington, VA 22217

Office of Naval Research  
Code 438  
Arlington, VA 22217

Office of Naval Research  
Code 1021P (ONRL)  
Arlington, VA 22217 6 Copies

Dr. J. L. Potter  
Deputy Director, Technology  
von Karman Gas Dynamics Facility  
Arnold Air Force Station, TN 37389

Professor J. C. Wu  
Georgia Institute of Technology  
School of Aerospace Engineering  
Atlanta, GA 30332

Library  
Aerojet-General Corporation  
6352 North Irwindale Avenue  
Azusa, CA 91702

NASA Scientific and Technical  
Information Facility  
P. O. Box 8757  
Baltimore/Washington International Airport  
Maryland 21240

Dr. S. A. Berger  
University of California  
Department of Mechanical Engineering  
Berkeley, CA 94720

Professor A. J. Chorin  
University of California  
Department of Mathematics  
Berkeley, CA 94720

Professor M. Holt  
University of California  
Department of Mechanical Engineering  
Berkeley, CA 94720

Dr. L. Talbot  
University of California  
Department of Mechanical Engineering  
Berkeley, CA 94720

Dr. H. R. Chaplin  
Code 16  
David W. Taylor Naval Ship Research  
and Development Center  
Bethesda, MD 20084

Code 1800  
David W. Taylor Naval Ship Research  
and Development Center  
Bethesda, MD 20084

Code 5643  
David W. Taylor Naval Ship Research  
and Development Center  
Bethesda, MD 20084

Dr. G. R. Inger  
Virginia Polytechnic Institute  
and State University  
Department of Aerospace Engineering  
Blacksburg, VA 24061

Professor A. H. Nayfeh  
Virginia Polytechnic Institute  
and State University  
Department of Engineering Science  
and Mechanics  
Blacksburg, VA 24061

Indiana University  
School of Applied Mathematics  
Bloomington, IN 47401

Director  
Office of Naval Research Branch Office  
495 Summer Street  
Boston, MA 02210

Supervisor, Technical Library Section  
Thiokol Chemical Corporation  
Wasatch Division  
Brigham City, UT 84302

Dr. G. Hall  
State University of New York at Buffalo  
Faculty of Engineering and  
Applied Science  
Fluid and Thermal Sciences Laboratory  
Buffalo, NY 14214

Mr. R. J. Vidal  
Calspan Corporation  
Aerodynamics Research Department  
P. O. Box 235  
Buffalo, NY 14221

Professor R. F. Probst  
Massachusetts Institute of Technology  
Department of Mechanical Engineering  
Cambridge, MA 02139

Director  
Office of Naval Research Branch Office  
536 South Clark Street  
Chicago, IL 60605

Code 753  
Naval Weapons Center  
China Lake, CA 93555

Mr. J. Marshall  
Code 4063  
Naval Weapons Center  
China Lake, CA 93555

Professor R. T. Davis  
University of Cincinnati  
Department of Aerospace Engineering  
and Applied Mechanics  
Cincinnati, OH 45221

Library MS 60-3  
NASA Lewis Research Center  
21000 Brookpark Road  
Cleveland, OH 44135

Dr. J. D. Anderson, Jr.  
Chairman, Department of Aerospace  
Engineering  
College of Engineering  
University of Maryland  
College Park, MD 20742

Professor W. L. Melnik  
University of Maryland  
Department of Aerospace Engineering  
Glenn L. Martin Institute of Technology  
College Park, MD 20742

Professor O. Burggraf  
Ohio State University  
Department of Aeronautical and  
Astronautical Engineering  
1314 Kinnear Road  
Columbus, OH 43212

Technical Library  
Naval Surface Weapons Center  
Dahlgren Laboratory  
Dahlgren, VA 22448

Dr. F. Moore  
Naval Surface Weapons Center  
Dahlgren Laboratory  
Dahlgren, VA 22448

Technical Library 2-51131  
LTV Aerospace Corporation  
P. O. Box 5907  
Dallas, TX 75222

Library, United Aircraft Corporation  
Research Laboratories  
Silver Lane  
East Hartford, CT 06108

Technical Library  
AVCO- Everett Research Laboratory  
2385 Revere Beach Parkway  
Everett, MA 02149

Professor G. Moretti  
Polytechnic Institute of New York  
Long Island Center  
Department of Aerospace Engineering  
and Applied Mechanics  
Route 110  
Farmingdale, NY 11735

Professor S. G. Rubin  
Polytechnic Institute of New York  
Long Island Center  
Department of Aerospace Engineering  
and Applied Mechanics  
Route 110  
Farmingdale, NY 11735

Technical Documents Center  
Army Mobility Equipment R&D Center  
Building 315  
Fort Belvoir, VA 22060

Dr. W. R. Briley  
Scientific Research Associates, Inc.  
P. O. Box 498  
Glastonbury, CT 06033

Library (MS 185)  
NASA Langley Research Center  
Langley Station  
Hampton, VA 23665

Dr. S. Nadir  
Northrop Corporation  
Aircraft Division  
3901 West Broadway  
Hawthorne, CA 90250

Professor A. Chapmann  
Chairman, Mechanical Engineering  
Department  
William M. Rice Institute  
Box 1892  
Houston, TX 77001

Dr. F. Lane  
KLD Associates, Inc.  
7 High Street  
Huntington, NY 11743

Technical Library  
Naval Ordnance Station  
Indian Head, MD 20640

Professor D. A. Caughey  
Cornell University  
Sibley School of Mechanical and  
Aerospace Engineering  
Ithaca, NY 14853

Professor E. L. Resler  
Cornell University  
Sibley School of Mechanical and  
Aerospace Engineering  
Ithaca, NY 14853

Professor S. F. Shen  
Cornell University  
Sibley School of Mechanical and  
Aerospace Engineering  
Ithaca, NY 14853



Library  
Midwest Research Institute  
425 Volker Boulevard  
Kansas City, MO 64110

Dr. M. M. Hafez  
Flow Research, Inc.  
P. O. Box 5040  
Kent, WA 98031

Dr. E. M. Murman  
Flow Research, Inc.  
P. O. Box 5040  
Kent, WA 98031

Dr. S. A. Orszag  
Cambridge Hydrodynamics, Inc.  
54 Baskin Road  
Lexington, MA 02173

Professor T. Cebeci  
California State University, Long Beach  
Mechanical Engineering Department  
Long Beach, CA 90840

Mr. J. L. Hess  
Douglas Aircraft Company  
3855 Lakewood Boulevard  
Long Beach, CA 90808

Dr. H. K. Cheng  
University of Southern California,  
University Park  
Department of Aerospace Engineering  
Los Angeles, CA 90007

Professor J. D. Cole  
University of California  
Mechanics and Structures Department  
School of Engineering and Applied  
Science  
Los Angeles, CA 90024

Engineering Library  
University of Southern California  
Box 77929  
Los Angeles, CA 90007

Dr. C. -M. Ho  
University of Southern California,  
University Park  
Department of Aerospace Engineering  
Los Angeles, CA 90007

Dr. T. D. Taylor  
The Aerospace Corporation  
P. O. Box 92957  
Los Angeles, CA 90009

Commanding Officer  
Naval Ordnance Station  
Louisville, KY 40214

Mr. B. H. Little, Jr.  
Lockheed-Georgia Company  
Department 72-74, Zone 369  
Marietta, GA 30061

Dr. C. Cook  
Stanford Research Institute  
Menlo Park, CA 94025

Professor E. R. G. Eckert  
University of Minnesota  
241 Mechanical Engineering Building  
Minneapolis, MN 55455

Library  
Naval Postgraduate School  
Monterey, CA 93940

McGill University  
Supersonic-Gas Dynamics Research  
Laboratory  
Department of Mechanical Engineering  
Montreal 12, Quebec, Canada

Librarian  
Engineering Library, 127-223  
Radio Corporation of America  
Morristown, NJ 07960

Dr. S. S. Stahara  
Nielsen Engineering & Research, Inc.  
510 Clyde Avenue  
Mountain View, CA 94043

Engineering Societies Library  
345 East 47th Street  
New York, NY 10017

Professor A. Jameson  
New York University  
Courant Institute of Mathematical  
Sciences  
251 Mercer Street  
New York, NY 10012



Professor G. Miller  
New York University  
Department of Applied Science  
26-36 Stuyvesant Street  
New York, NY 10003

Office of Naval Research  
New York Area Office  
715 Broadway - 5th Floor  
New York, NY 10003

Dr. A. Vaglio-Laurin  
New York University  
Department of Applied Science  
26-36 Stuyvesant Street  
New York, NY 10003

Professor S. Weinbaum  
Research Foundation of the City  
University of New York on behalf  
of the City College  
1411 Broadway  
New York, NY 10018

Librarian, Aeronautical Library  
National Research Council  
Montreal Road  
Ottawa 7, Canada

Lockheed Missiles and Space Company  
Technical Information Center  
3251 Hanover Street  
Palo Alto, CA 94304

Director  
Office of Naval Research Branch Office  
1030 East Green Street  
Pasadena, CA 91106

California Institute of Technology  
Engineering Division  
Pasadena, CA 91109

Library  
Jet Propulsion Laboratory  
4800 Oak Grove Drive  
Pasadena, CA 91103

Professor H. Liepmann  
California Institute of Technology  
Department of Aeronautics  
Pasadena, CA 91109

Mr. L. I. Chasen, MGR-MSD Lib.  
General Electric Company  
Missile and Space Division  
P. O. Box 8555  
Philadelphia, PA 19101

Mr. P. Dodge  
Airesearch Manufacturing Company  
of Arizona  
Division of Garrett Corporation  
402 South 36th Street  
Phoenix, AZ 85034

Technical Library  
Naval Missile Center  
Point Mugu, CA 93042

Professor S. Bogdonoff  
Princeton University  
Gas Dynamics Laboratory  
Department of Aerospace and  
Mechanical Sciences  
Princeton, NJ 08540

Professor S. I. Cheng  
Princeton University  
Department of Aerospace and  
Mechanical Sciences  
Princeton, NJ 08540

Dr. J. E. Yates  
Aeronautical Research Associates  
of Princeton, Inc.  
50 Washington Road  
Princeton, NJ 08540

Professor J. H. Clarke  
Brown University  
Division of Engineering  
Providence, RI 02912

Professor J. T. C. Liu  
Brown University  
Division of Engineering  
Providence, RI 02912

Professor L. Sirovich  
Brown University  
Division of Applied Mathematics  
Providence, RI 02912

Dr. P. K. Dai (R1/2178)  
TRW Systems Group, Inc.  
One Space Park  
Redondo Beach, CA 90278

Redstone Scientific Information  
Center  
Chief, Document Section  
Army Missile Command  
Redstone Arsenal, AL 35809

U.S. Army Research Office  
P. O. Box 12211  
Research Triangle, NC 27709

Professor M. Lessen  
The University of Rochester  
Department of Mechanical Engineering  
River Campus Station  
Rochester, NY 14627

Editor, Applied Mechanics Review  
Southwest Research Institute  
8500 Culebra Road  
San Antonio, TX 78228

Library and Information Services  
General Dynamics-CONVAIR  
P. O. Box 1128  
San Diego, CA 92112

Dr. R. Magnus  
General Dynamics-CONVAIR  
Kearny Mesa Plant  
P. O. Box 80847  
San Diego, CA 92138

Mr. T. Brundage  
Defense Advanced Research  
Projects Agency  
Research and Development  
Field Unit  
APO 146, Box 271  
San Francisco, CA 96246

Office of Naval Research  
San Francisco Area Office  
760 Market Street - Room 447  
San Francisco, CA 94102

Library  
The Rand Corporation  
1700 Main Street  
Santa Monica, CA 90401

Department Librarian  
University of Washington  
Department of Aeronautics and  
Astronautics  
Seattle, WA 98105

Dr. P. E. Rubbert  
Boeing Commercial Airplane Company  
P. O. Box 3707  
Seattle, WA 98124

Mr. R. Feldhuhn  
Naval Surface Weapons Center  
White Oak Laboratory  
Silver Spring, MD 20910

Dr. G. Heiche  
Naval Surface Weapons Center  
Mathematical Analysis Branch  
Silver Spring, MD 20910

Librarian  
Naval Surface Weapons Center  
White Oak Laboratory  
Silver Spring, MD 20910

Dr. J. M. Solomon  
Naval Surface Weapons Center  
White Oak Laboratory  
Silver Spring, MD 20910

Professor J. H. Ferziger  
Stanford University  
Department of Mechanical Engineering  
Stanford, CA 94305

Professor K. Karamcheti  
Stanford University  
Department of Aeronautics and  
Astronautics  
Stanford, CA 94305

Professor M. van Dyke  
Stanford University  
Department of Aeronautics and  
Astronautics  
Stanford, CA 94305

Engineering Library  
McDonnell Douglas Corporation  
Department 218, Building 101  
P. O. Box 516  
St. Louis, MO 63166

Dr. R. J. Hakkinen  
McDonnell Douglas Corporation  
Department 222  
P. O. Box 516  
St. Louis, MO 63166

Dr. R. P. Heinisch  
Honeywell, Inc.  
Systems and Research Division -  
Aerospace Defense Group  
2345 Walnut Street  
St. Paul, MN 55113

Professor R. G. Stoner  
Arizona State University  
Department of Physics  
Tempe, AZ 85721

Dr. N. Malmuth  
Rockwell International  
Science Center  
1049 Camino Dos Rios  
P. O. Box 1085  
Thousand Oaks, CA 91360

Rockwell International  
Science Center  
1049 Camino Dos Rios  
P. O. Box 1085  
Thousand Oaks, CA 91360

The Library  
University of Toronto  
Institute of Aerospace Studies  
Toronto 5, Canada

Professor W. R. Sears  
University of Arizona  
Aerospace and Mechanical Engineering  
Tucson, AZ 85721

Professor A. R. Seebass  
University of Arizona  
Department of Aerospace and  
Mechanical Engineering  
Tucson, AZ 85721

Dr. S. M. Yen  
University of Illinois  
Coordinated Science Laboratory  
Urbana, IL 61801

Dr. K. T. Yen  
Code 3015  
Naval Air Development Center  
Warminster, PA 18974

Air Force Office of Scientific  
Research (SREM)  
Building 1410, Bolling AFB  
Washington, DC 20332

Chief of Research & Development  
Office of Chief of Staff  
Department of the Army  
Washington, DC 20310

Library of Congress  
Science and Technology Division  
Washington, DC 20540

Director of Research (Code RR)  
National Aeronautics and  
Space Administration  
600 Independence Avenue, SW  
Washington, DC 20546

Library  
National Bureau of Standards  
Washington, DC 20234

National Science Foundation  
Engineering Division  
1800 G Street, NW  
Washington, DC 20550

Mr. W. Koven (AIR 03E)  
Naval Air Systems Command  
Washington, DC 20361

Mr. R. Siewert (AIR 320D)  
Naval Air Systems Command  
Washington, DC 20361

Technical Library Division (AIR 604)  
Naval Air Systems Command  
Washington, DC 20361



Page 8

Code 2627  
Naval Research Laboratory  
Washington, DC 20375

SEA 03512  
Naval Sea Systems Command  
Washington, DC 20362

SEA 09G3  
Naval Sea Systems Command  
Washington, DC 20362

Dr. A. L. Slafkosky  
Scientific Advisor  
Commandant of the Marine Corps  
(Code AX)  
Washington, DC 20380

Director  
Weapons Systems Evaluation Group  
Washington, DC 20305

Dr. P. Baronti  
General Applied Science  
Laboratories, Inc.  
Merrick and Stewart Avenues  
Westbury, NY 11590

Bell Laboratories  
Whippany Road  
Whippany, NJ 07981

Chief of Aerodynamics  
AVCO Corporation  
Missile Systems Division  
201 Lowell Street  
Wilmington, MA 01887

Research Library  
AVCO Corporation  
Missile Systems Division  
201 Lowell Street  
Wilmington, MA 01887

AFAPL (APRC)  
AB  
Wright Patterson, AFB, OH 45433

Dr. Donald J. Harney  
AFFDL/FX  
Wright Patterson AFB, OH 45433